

Accepted Manuscript

Design, synthesis and antitumor study of a series of *N*-Cyclic sulfamoylaminoethyl substituted 1,2,5-oxadiazol-3-amines as new indoleamine 2, 3-dioxygenase 1 (IDO1) inhibitors

Shulun Chen, Wei Guo, Xiaohua Liu, Pu Sun, Yi Wang, Chunyong Ding, Linghua Meng, Ao Zhang

PII: S0223-5234(19)30564-1

DOI: <https://doi.org/10.1016/j.ejmech.2019.06.037>

Reference: EJMECH 11440

To appear in: *European Journal of Medicinal Chemistry*

Received Date: 22 April 2019

Revised Date: 13 June 2019

Accepted Date: 13 June 2019

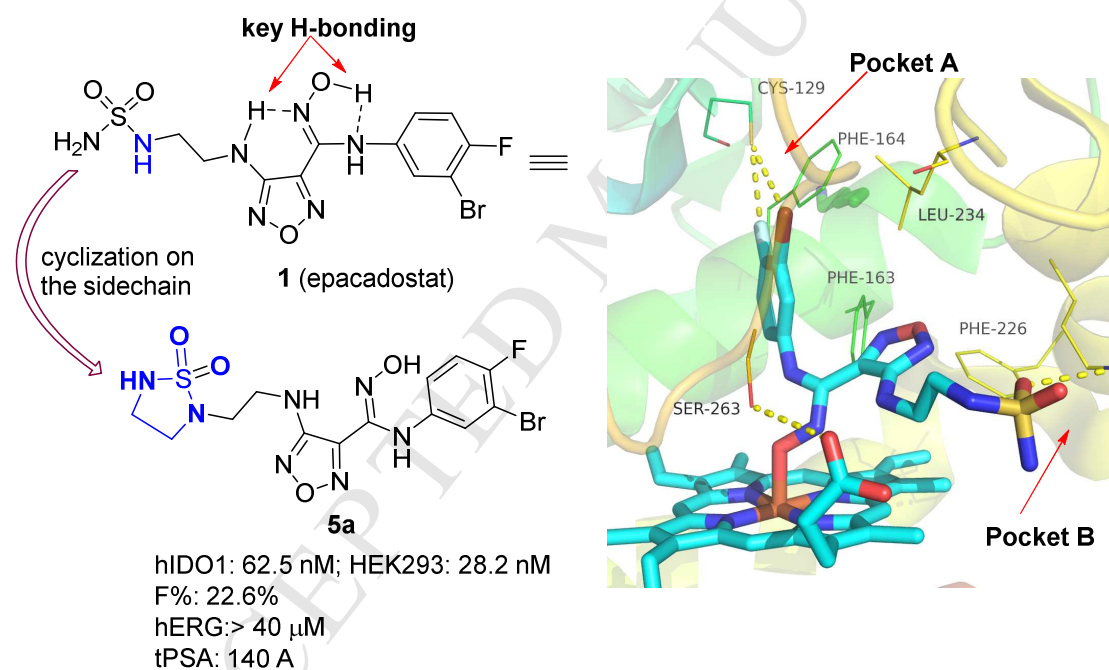
Please cite this article as: S. Chen, W. Guo, X. Liu, P. Sun, Y. Wang, C. Ding, L. Meng, A. Zhang, Design, synthesis and antitumor study of a series of *N*-Cyclic sulfamoylaminoethyl substituted 1,2,5-oxadiazol-3-amines as new indoleamine 2, 3-dioxygenase 1 (IDO1) inhibitors, *European Journal of Medicinal Chemistry* (2019), doi: <https://doi.org/10.1016/j.ejmech.2019.06.037>.

This is a PDF file of an unedited manuscript that has been accepted for publication. As a service to our customers we are providing this early version of the manuscript. The manuscript will undergo copyediting, typesetting, and review of the resulting proof before it is published in its final form. Please note that during the production process errors may be discovered which could affect the content, and all legal disclaimers that apply to the journal pertain.



Graphic Abstract:**Design, Synthesis and Antitumor Study of a Series of *N*-Cyclic Sulfamoylaminoethyl Substituted 1,2,5-Oxadiazol-3-amines as New Indoleamine 2,3-dioxygenase 1 (IDO1) Inhibitors**

Shulun Chen,^{1,3} Wei Guo,^{2,3} Xiaohua Liu,^{1,3} Pu Sun,² Yi Wang,² Chunyong Ding,^{1,3} Linghua Meng,^{2,3,*} Ao Zhang^{1,3,4,*}



Highlights:

- IDO1 plays a key role in tryptophan catabolism and in immune tolerance.
- Epacadostat is the most advanced IDO1 inhibitor, but its phase III trial was failed.
- A series of analogues of epacadostat was designed and further optimized.
- **5a** displayed significant potency against hIDO1 and hIDO1 expressed cancer cells.
- **5a** was ineffective as single agent in the CT-26 syngeneic xenograft model.
- Combination with mPD-1 showed elevated efficacy and prolonged median life span.

Design, Synthesis and Antitumor Study of a Series of *N*-Cyclic Sulfamoylaminoethyl Substituted 1,2,5-Oxadiazol-3-amines as New Indoleamine 2, 3-dioxygenase 1 (IDO1) Inhibitors

Shulun Chen,^{1,3} Wei Guo,^{2,3} Xiaohua Liu,^{1,3} Pu Sun,² Yi Wang,² Chunyong Ding,^{1,3} Linghua Meng,^{2,3,*} Ao Zhang^{1,3,4,*}

¹CAS Key Laboratory of Receptor Research, Shanghai Institute of *Materia Medica* (SIMM), Chinese Academy of Sciences, Shanghai 201203, China

²Division of Anti-tumor Pharmacology, Shanghai Institute of *Materia Medica* (SIMM), Chinese Academy of Sciences, Shanghai 201203, China.

³University of Chinese Academy of Sciences, Beijing100049, China.

⁴School of Life Science and Technology, ShanghaiTech University, Shanghai 201210, China

Abstract

Indoleamine 2, 3-dioxygenase 1 (IDO1) plays a key role in tryptophan catabolism which is an important mechanism in immune tolerance. The small molecule epacadostat is the most advanced IDO1 inhibitor, but its phase III trials as a single agent or in combinations with PD-1 antibody failed to show appreciable objective responses. To gain more insight on the antitumor efficacy of IDO1 inhibitors, we have designed a series of analogues of epacadostat by incorporating a cyclic aminosulfonamide moiety as the sidechain capping functionality. Compound **5a** was found to display significant potency against recombinant hIDO1 and hIDO1 expressed HEK293 cancer cells. This compound has improved physico-chemical properties, acceptable PK parameters as well as optimal cardiac safety. Similar to epacadostat, **5a** is ineffective as single agent in the CT-26 syngeneic xenograft model, however, the combination of **5a** with PD-1 antibody showed both elevated tumor growth inhibition and prolonged median life span.

Keywords: Indoleamine 2,3-dioxygenase; Immunotherapy; Oxadiazole; PD-1; Life span.

1. Introduction

The rapid advances in oncology immunotherapy, highlighted by checkpoint inhibitors targeting cytotoxic T lymphocyte associated protein 4 (CTLA-4) and the programmed death receptor 1/ligand 1 (PD-1/PD-L1), have substantially revolutionized our vision and treatment options on advanced human cancers.¹⁻² Among which, the anti-CTLA-4 antibody (ipilimumab) and anti-PD1 antibody (pembrolizumab and nivolumab) approved by FDA, have demonstrated impressive therapeutic effects on patients.³⁻⁵ Compared to other anticancer modalities (irradiation, chemotherapy, and targeted therapy) that exert their therapeutic effects via directly suppressing/killing proliferating cancer cells, cancer immunotherapy can recognize and eliminate tumor cells by restoring and even activating the patients' native immune system,⁶ thus affording better control of tumor growth with sustainable therapeutic responses. However, clinic studies have shown that a significant majority of cancer patients do not respond to the existing checkpoint inhibitors, and the emergence of acquired resistance is more and more commonly observed in patients who initially responded.⁷⁻⁸ Therefore, there is a need to develop new immunotherapies either to be used alone or in combination with existing checkpoint inhibitors.

In addition to CTLA-4 and PD-1/PD-L1, indoleamine 2, 3-dioxygenase (IDO1), an enzyme with immunosuppressive property was found being overexpressed in a wide variety of human tumors.⁹ IDO1 catalyzes the initial and rate-limiting step of tryptophan (TRP) catabolism via the kynurenine (Kyn) pathway, an important mechanism in immune tolerance¹⁰⁻¹². IDO1 oxidizes the essential amino acid

tryptophan to *N*-formyl kynurenine (NFK) which is further converted to Kyn and other bioactive metabolites¹¹. Tryptophan depletion activates general control non-derepressible 2 (GCN2) and represses mechanistic target of rapamycin kinase (mTOR). Furthermore, biologically active metabolites in kynurenine pathway, such as Kyn, activate the aryl hydrocarbon receptor (AhR). IDO1 is overexpressed in cancer cell and the antigen presenting dendritic cell in tumor microenvironment. The cancer cells overexpressing IDO1 can evade immune surveillance, and the transcriptional factor AhR participates in cancer immune escape by binding to the IDO product Kyn.¹³⁻¹⁶ Considering the important role of IDO1 in immune tolerance¹⁵, inhibition of IDO1 has become an exciting approach to cancer immunotherapy. A number of small-molecule IDO1 inhibitors have been reported,^{6, 10, 17-25} with a few being extensively investigated in clinical trials, including **1** (epacadostat, INCB024360⁶), **2** (BMS-986205²⁶), **3** (navoximod, GDC-0919²⁷) and **4** (PF-06840003²⁰) (Figure 1). Unfortunately, clinical trials of IDO1 inhibitors as monotherapy have suffered from setbacks recently since the pronounced tumor reduction of epacadostat observed in preclinical studies was not confirmed in phase I and II trials.²⁸⁻²⁹ Alternatively, combination regimens with other immunotherapies, chemo-therapies or chemo-radiation are being extensively pursued.³⁰⁻³² Both IDO1 and PD-L1 are co-expressed in tumor cells. A recent phase II trial demonstrated that inhibition of PD-1 has limited activity in selected advanced soft-tissue sarcoma, which might be associated with an immunosuppressive tumor microenvironment resulting from macrophage infiltration and IDO1 pathway activation.³³ In addition, the ratio of

Kyn/tryptophan was found to be increased during PD-1 antibody treatment, indicating that IDO1 activation might be related to the limited efficacy of PD-1/PD-L1 treatment. Therefore, a synergistic effect is expected by combination of IDO1 inhibitors with PD-1/PD-L1 blockades. Intriguingly, a recent phase III ECHO 301 trial testing the combination of IDO1 inhibitor epacadostat with PD-1 antibody pembrolizumab in melanoma failed to show superior objective responses compared to pembrolizumab alone.³⁴ Although the clinical readout from a single trial is not a definitive determinant for the field, development of new IDO1 inhibitors and combinations with different checkpoint inhibitors in well-defined patients together with precise trial design are urgently needed.

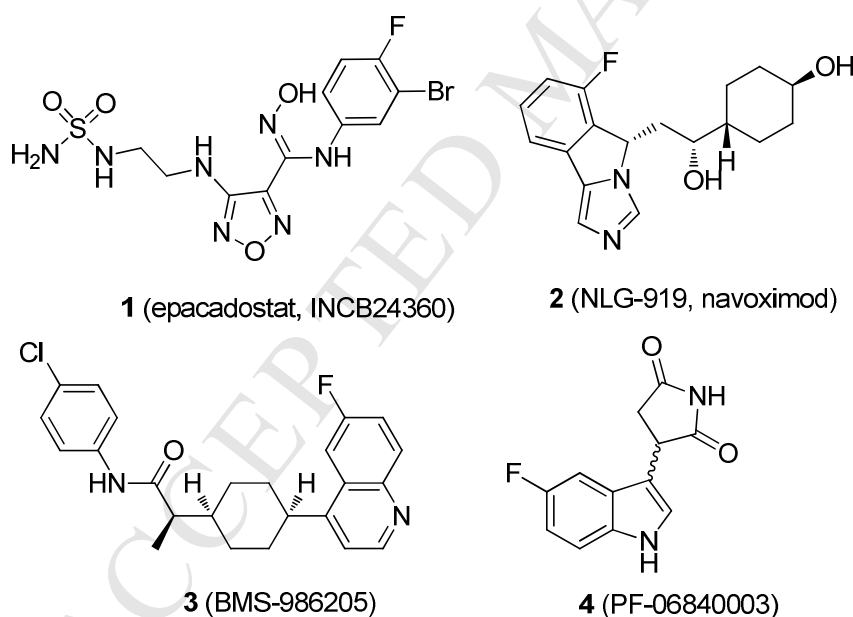


Figure 1. Representative clinical IDO1 inhibitors.

To gain more insight on the tumor-suppressing effect of IDO1 inhibitors, we recently conducted a structural modification campaign on the clinical IDO1 inhibitor epacadostat, by cyclizing the sulfamoylamine component of the sidechain to explore the electronic and steric effects on IDO1 activity. Herein, we report on the SAR and

antitumor activity of these new IDO1 inhibitors both as monotherapy and in combination with PD-1 antibody blockade.

2. Results and discussion

2.1. Structural analysis and new inhibitor design

1,2,5-Oxadiazole **1**⁶, developed by Incyte Corp is the most advanced IDO1 inhibitor in clinical trials. It has moderate inhibitory potency (IC_{50} , 73 nM) against IDO1 enzyme and high inhibitory potency in HeLa cells (IC_{50} , 7.4 nM). The co-crystal structure³⁵ of hIDO1 in complex with **1** (PDB code: 5WN8) shows that the oxime oxygen forms the key hexa-coordination with the heme iron while the halogenated phenyl group forms a favorable fluorine–sulfur contact with C129 and occupies the hydrophobic pocket A situating above the heme. The sulfamoylamino ethylene sidechain projects out to reach the pocket B. The central 1,2,5-oxadiazole moiety is stabilized by F163, L234, and F226. Although compound **1** shows significant inhibitory effects on IDO1 catalytic activity, and appreciable tumor growth inhibition in immunocompetent C57BL/6 mouse syngeneic models of several cancer types,^{6,36} its chemical structure lacks optimal drug-like properties (e.g. the number of H-bond donor/acceptor >10; PSA > 140 Å) due to the co-existence of several polar functional groups including hydroxamidine and sulfamoylamine. A close examination of the interaction of the sulfamoylamino ethylene sidechain suggests that the proposed allosteric pocket B is not fully occupied and the secondary NH in the sulfamoylamine component is not involved in the H-bonding network (Figure 2). In this regard, we decide to cyclize the sulfamoylamine component aiming to fully occupy the pocket B

and to balance the PK properties by adjusting electronic and steric effects of the cyclic congeners. In the meantime, the polar hydroxamidine functionality is left intact to maintain the key intramolecular H-bonding network that forces the amidine C=N double bond to hold a *cis* conformation (Figure 2).

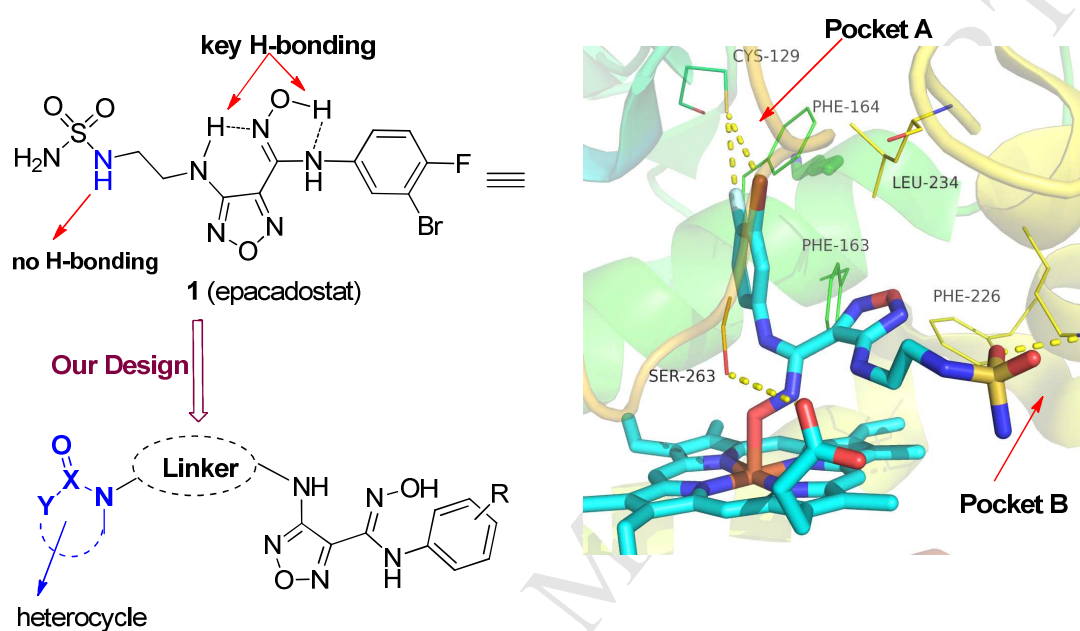


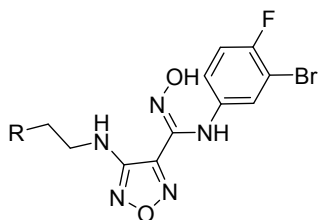
Figure 2. Co-crystal structure of **1** with IDO1 and our design of new IDO1 inhibitors.

2.2. Structure-activity relationship analysis

All the new compounds were assayed for their activity against hIDO1 enzyme and active compounds were further tested for their activity in HEK293 cells over-expressing hIDO1. The clinical compound **1** was used as comparison. As shown in Table 1, we first evaluated a series of analogues bearing a five- or six-membered cyclic aminosulfonamide as the capping group of the sidechain. Compared to the parent compound **1**, compound **5a**, formed by directly cyclization of the sulfamoylamine moiety of **1** into a five-membered heterocycle, showed slightly lower but still compatible potency against hIDO1 in both biochemical and cellular assays with IC₅₀ values of 62.5 and 28.2 nM, respectively. Further masking the terminal NH

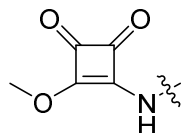
with a methyl group yielded compound **5b**, showing nearly the same potency as that of **5a**. These results suggested that both the NH₂ and NH groups in the aminosulfonamide component of **1** are not substantially requested for the interaction with hIDO1. However, a larger six-membered analog **5c** lost activities against the recombinant hIDO1 with an IC₅₀ greater than 1 μM, suggesting that the size of the heterocycle and the steric effect of the capping group are crucial to interact with hIDO1. Interestingly, compound **5d** lacking the cyclic NH moiety of **5a** showed even higher potency in both biochemical and cellular assays with IC₅₀ values of 46.5 and 21.4 nM, respectively. This compound is slightly more potent than the reference compound **1** (62.6 and 28.2 nM, respectively in both assays), though the difference is not statistically significant. Replacing the sulfonyl group in **5a** by carbonyl group led to compound **5e**, completely lost the activity against hIDO1. However, the analog **5f** retained good potency in both biochemical and cellular assays with IC₅₀ values of 71.5 and 16.8 nM, respectively. Compared to the parent compound **1**, the retained good potency of **5d** and **5f** suggested that the H-bonding donor in the sidechain terminal group is not necessary, which may benefit the PK-related physico-chemical properties. This analysis was further confirmed by the isoxazolidinone **5g** and dihydroisoxazole **5f**, both retained reasonable potency in both assays. The phenyl fused cyclic analogs **5i** and **5j** were inactive to hIDO1, likely due to their steric and electronic effects. Interestingly, compound **6** bearing a 4-methoxycyclobut-3-ene-1,2-dione-3-amino moiety as the sidechain capping group also retained moderate potency against hIDO1, only 3.3-fold less potent than **1** (138 vs 40.9 nM).

Table 1.Biochemical and cellular potency of cyclic aminosulfonamides as new IDO1 inhibitors^a



Compound	R	IC ₅₀ (nM)	
		hIDO-1	HEK293
1		40.9	12.6 ± 1.0
5a		62.5	28.2 ± 2.2
5b		56.2	33.0 ± 0.8
5c		>1000	NT ^b
5d		46.5	21.4 ± 0.8
5e		>1000	NT ^b
5f		71.5	16.8 ± 2.0
5g		115	72.9 ± 4.9
5h		94.5	73.2 ± 1.4
5i		817	NT ^b
5j		>1000	NT ^b

6



138

NT^b

^aThe IC₅₀ values are obtained from two separate experiments. ^bNT = not tested.

Starting from cyclic aminosulfonamide **5a**, we next screened a small series of aryl groups with different substitution patterns to determine the electronic and steric tolerance of the pocket A. As shown in Table 2, the 4-fluoro group of phenyl is critical for IDO1 interaction and other substituents (e.g. OCH₂CF₃ in **7a**, SO₂CH₂CH₃ in **7b**, SeCH₂CH₃ in **7c**) completely abolished the activity against IDO1 with IC₅₀ values greater than 1 μM. Keeping the 4-fluoro intact and replacement of the 3-bromo with chloro or introducing an additional halogen atom on the 5-position of the phenyl led to compounds **7d-f**, all showing much reduced potency against hIDO1 with IC₅₀ value ranging between 112 nM to >1 μM.

Table 2.

The hIDO1 activity of cyclic aminosulfonamides with different aryl substituents^a

Compound	R ¹	R ²	R ³	hIDO-1 IC ₅₀ (nM)
5a	Br	F	H	62.5
7a	Br	OCH ₂ CF ₃	H	>1000
7b	Br	SO ₂ CH ₂ CH ₃	H	>1000
7c	Br	SeCH ₂ CH ₃	H	>1000
7d	Cl	F	H	112
7e	Cl	F	Cl	304

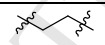
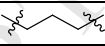
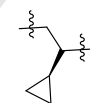
7f	Br	F	Br	>1000
-----------	----	---	----	-------

^aThe IC₅₀ values are obtained from two separate experiments.

We also used a few alkyl linkers bearing different length and steric effect to replace the ethylene linkage in cyclic aminosulfonamide **5a**. As shown in Table 3, extending the ethylene linker in **5a** to a three-methylene linker in **8a** led to 3~4-fold reduction in the potency against hIDO1 with an IC₅₀ value of 217 nM. Further reduced activity was observed for the steric linker as in **8b** and **8c**. The 3-fold higher potency for **8c** over **8b** (221 vs 696 nM) further confirms the ethylene unit as the optimum linkage.

Table 3.

The hIDO1 enzymatic activity of cyclic aminosulfonamides with different linkers^a

Compound	R	hIDO-1 IC ₅₀ (nM)
5a		62.5
8a		217
8b		696
8c		221

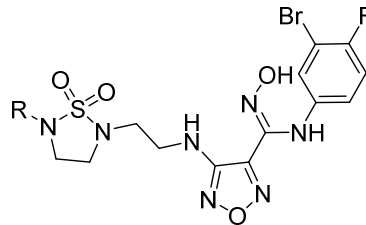
^aThe IC₅₀ values are obtained from two separate experiments.

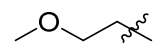
Since no improvement was achieved by modifying the linker and the aryl substituents, we then optimized the *N*-substituent of the cyclic aminosulfonamido component in **5a**. As shown in Table 4, we first introduced a series of water-soluble groups as *N*-substituents. Compared to **5a**, *N*-(2-MeO)ethyl substituted compound **9a**

showed slightly lower potency (78.5 vs 62.5 nM) against hIDO1 in the biochemical assay, whereas the potency in IDO1-expressed HEK293 cells was slightly improved (22.2 vs 28.2 nM). One methylene longer *N*-substituent in **9b** led to 6-fold reduction in potency. *N*-(2-OH)-ethyl substituted **9c** showed nearly the same potency as **5a** in both biochemical and cellular assays with IC₅₀ values of 74.5 and 26.6 nM, respectively. No potency gain for the PEGlated analogue **9d** (284 nM). Reduced potency was observed as well for the *N*-((3-(hydroxymethyl)oxetan-3-yl)methyl) analogue **9e** (322 nM). Basic substituents as in **9f** and **9g** were introduced aiming to increase the aqueous solubility. Compared to **5a**, compound **9f** bearing dimethylamino ethyl as the *N*-substituent showed a 4-fold reduction in potency, whereas the morpholin-4-ylethyl substituted analogue **9g** showed compatible potency in both biochemical and cell assays with IC₅₀ values of 83.3 and 28.7 nM, respectively. Various aryl, heteroaryl and alkyl substituents were also tested and the corresponding compounds **9h-k** were 4- to 11-fold less potent than **5a**. The *N*-ethyl substituted analogues **9l** and **9m** bearing a terminal cabamoyl moiety also showed reduced potency against hIDO1.

Table 4.

N-Substituted cyclic aminosulfonamides as new IDO1 inhibitors



Compound	R	IC ₅₀ (nM)	
		hIDO-1	HEK 293
1	/	40.9	12.6 ± 1.0
5a	H	62.5	28.2 ± 2.2
9a		78.5	22.2 ± 6.2

9b		461	^a NT
9c		74.5	26.6 ± 4.5
9d		284	^a NT
9e		322	^a NT
9f		221	45.7 ± 8.3
9g		83.3	28.7 ± 5.0
9h		657	^a NT
9i		399	^a NT
9j		457	^a NT
9k		259	^a NT
9l		767	^a NT
9m		354	^a NT

^aNT = not tested. The IC₅₀ values are obtained from two separate experiments.

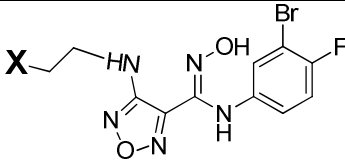
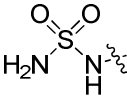
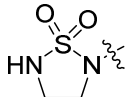
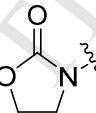
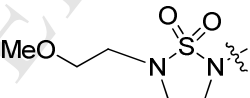
2.3. *hERG* potassium channel test

By balancing the biochemical and cellular potency as well as the structural diversity, compounds **5a**, **5d**, **5f** and **9a** were selected as the representative leads of corresponding subseries for further evaluation (Table 5). Compared to the parent compound **1**, all these new compounds showed similar potency, but more favorable polar surface area thus matching Veber's permeability rules (tPSA <140 Å). Since these compounds have high loading of *N*-atom, compared to most clinically approved

drugs, we then tested their inhibitory effects against the hERG potassium channel to exclude the potential effects on the cardiac arrhythmia. Fortunately, all these compounds showed IC_{50} values greater than 15 μM , indicating their optimal cardiac safety profile.

Table 5.

Inhibitory effects of new IDO1 inhibitors against hERG channel

Compound		hERG, IC_{50} (μM)	tPSA (\AA)
	X =		
1		>40	162.8
5a		>40	140.0
5d		17.27	128.0
5f		31.12	120.1
9a		16.63	140.4

2.4. Pharmacokinetic study

To further evaluate the developable potential of these new IDO1 inhibitors, the pharmacokinetic profile (PK) of the four new compounds was tested in SD rats dosed iv (1 mg/kg) and orally (3 mg/kg). As shown in Table 6, **5d** and **9a** showed poor oral bioavailability of 6.55% and 1.21%, respectively. However, **5a** showed a good oral bioavailability of 22.6% (reported data for **1**⁶: F(rat) = 11%). **5f** also displayed an

acceptable oral bioavailability of 13.9%. Both **5a** and **5f** showed moderate plasma clearance (40.3 and 51.0 mL/min/kg), respectively.

Table 6.

Pharmacokinetic profile of four compounds in SD rats^a

Compound	T _{1/2} (h)	AUC (h*ng/mL)		CL _{obs} (mL/min/kg)	V _{ss} _{obs} (ml/kg)	F(%)	
		AUC _{last}	AUC _{INF_obs}				
5a	p.o.	1.94	275	356	-	-	22.6
	i.v.	1.49	406	415	40.3	4295	
5d	p.o.	1.58	58.1	60.5	-	-	6.55
	i.v.	0.575	296	311	54.6	3016	
5f	p.o.	1.79	137	142	-	-	13.9
	i.v.	1.18	329	330	51.0	2557	
9a	p.o.	1.91	2.59	6.52	-	-	1.21
	i.v.	0.617	71.2	75.6	225	9835	

^aValues are the average of three runs. Vehicle: PO: DMSO/0.5%HPMC (5/95, v/v); iv: EtOH/PEG300/NaCl (10/40/50, v/v/v). CL, clearance; V_{ss}, volume of distribution; T_{1/2}, half-life; AUC, area under the plasma concentration time curve; F, oral bioavailability.

2.5. Antitumor activity of compound **5a** in CT-26 murine xenograft model

On the basis of its high potency against hIDO1, and acceptable PK parameters, compound **5a** was further investigated in vivo for its antitumor efficacy both as single agent and in combination with mPD-1 antibody (mouse PD-1 antibody, BioXCell, Cat# BE0146)³⁷ in a CT26 xenograft model in immunocompetent mice. Immunocompetent mice were treated with vehicle, compound **5a** (100 mg/kg, BID), clinical compound **1** (100 mg/kg, BID), anti-mPD-1 (10 mg/kg, BIW) or a combination of **5a** and antibody. As shown in Table 7 and Figure 3, treatment with **1** or **5a** alone showed marginal inhibition on tumor growth (TGI =19.4% and 7.3%,

respectively) indicating that monotherapy of either the clinical drug **1** or our new inhibitor **5a** is ineffective. Treatment with anti-mPD-1 showed moderate antitumor efficacy (TGI = 37.0%), which is better than both small molecules **1** and **5a**. As expected, combination of **5a** with the anti-PD1 antibody significantly enhanced the efficacy of the monotherapy, with a TGI of 47.4%. Moreover, no significant change in body weight was observed in combinatorial group compared to each monotherapy group during the 14-day treatment.

Table 7.

Inhibition of compound **5a** on tumor growth in the CT-26 syngeneic model

Treatment	Tumor Size (mm ³) ^a at PG-D14	T/C ^b (%)	TGI (%)	<i>p</i> value (one-way ANOVA) ^c
Vehicle	1557±256	--	--	--
1	1265±115	81.2	19.4	0.317
mPD-1	999±247	64.2	37.0	0.140
5a	1447±55	92.9	7.3	0.681
5a+mPD-1	842±148	54.1	47.4	0.030

^aMean ± SEM.

^bTumor growth inhibition is calculated by dividing the average tumor volume in the treated group by that in the vehicle control group (T/C).

^c*p* value was calculated with one-way-ANOVA by comparing treated group with vehicle group.

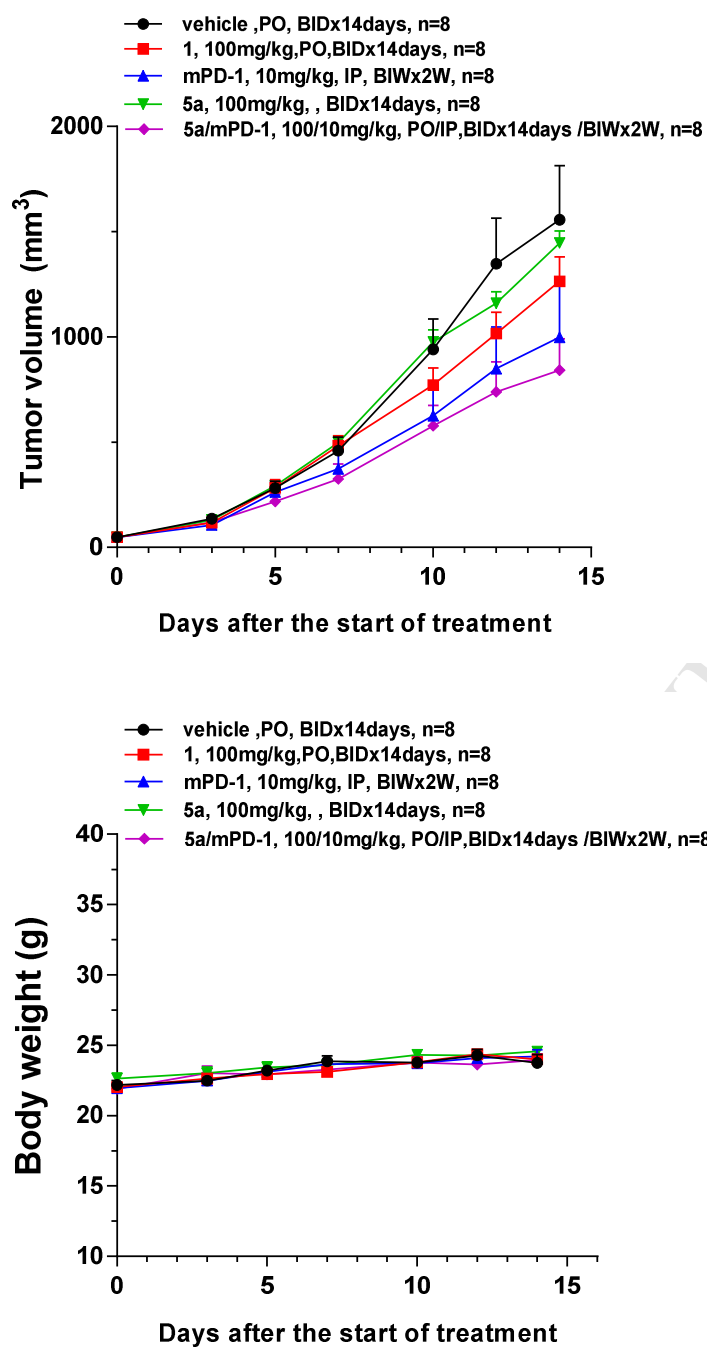


Figure 3. Tumor growth curve and change in body weights in female BALB/c mice bearing CT-26 xenografts. Data points represent mean of each group, error bars represent standard error of the mean (SEM).

Meanwhile, as shown in Table 8 and Figure 4, we further gauged the median survival time (MST) of each treatment group. It was found that mice treated with both small-molecule IDO1 inhibitors **1** and **5a** showed similar survival time to those in

control group (~20 d), while the mice treated with anti-PD1 antibody showed a slightly longer MST of 24 d. Significantly improved MST (> 26 d) was observed in mice in the combination groups ($P < 0.001$) with the ratio of increase in life-span (ILS) > 30%, indicating that combination of **5a** and anti-mPD-1 not only enhanced the antitumor efficacy and also extended the survival time of tumor-bearing mice.

Table 8.

The effects of **5a** or/and mPD-1 on the survival of tumor bearing mice

Group	Treatment	Mean (days)	MST ^c (days)	ILS ^d (%)	<i>p</i> value (Kaplan-Meier method)
1	Vehicle	20.5 ^a (16~24)	20	—	—
2	1	21.5 ^a (20~24)	20	0	^b 0.754
3	mPD-1	23.5 ^a (18~>26)	24	20	^b 0.036
4	5a	20.25 ^a (18~22)	20	0	^b 0.744
5	5a+mPD-1	25.25 ^a (22~>26)	>26	>30	^b 0.001

^aThe range of survival times.

^b*p* value when comparing each group with Group 1.

^cThe survival of all animals was followed and median survival time (MST) was calculated for each group.

^dThe increase in life-span (ILS) was calculated by dividing the MST of treatment group by the MST of the control group and was expressed as the percent increase over the life-span of animals in the control group.

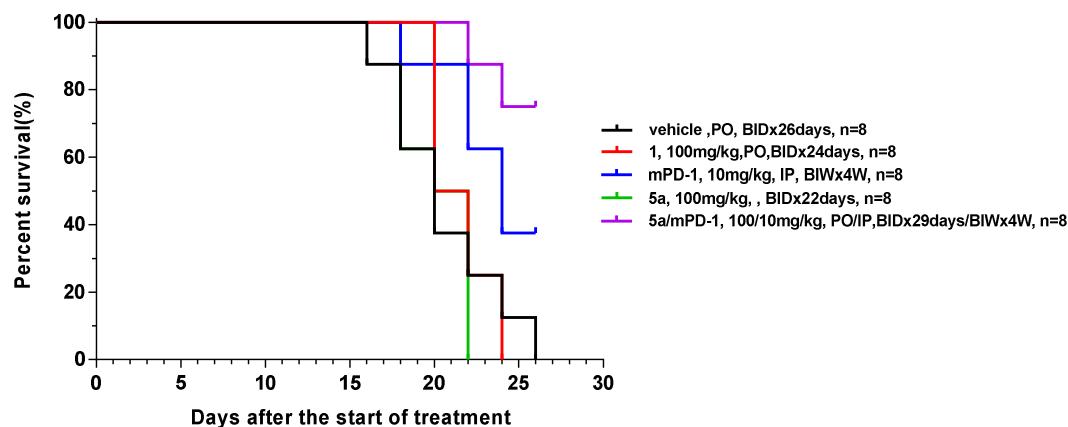
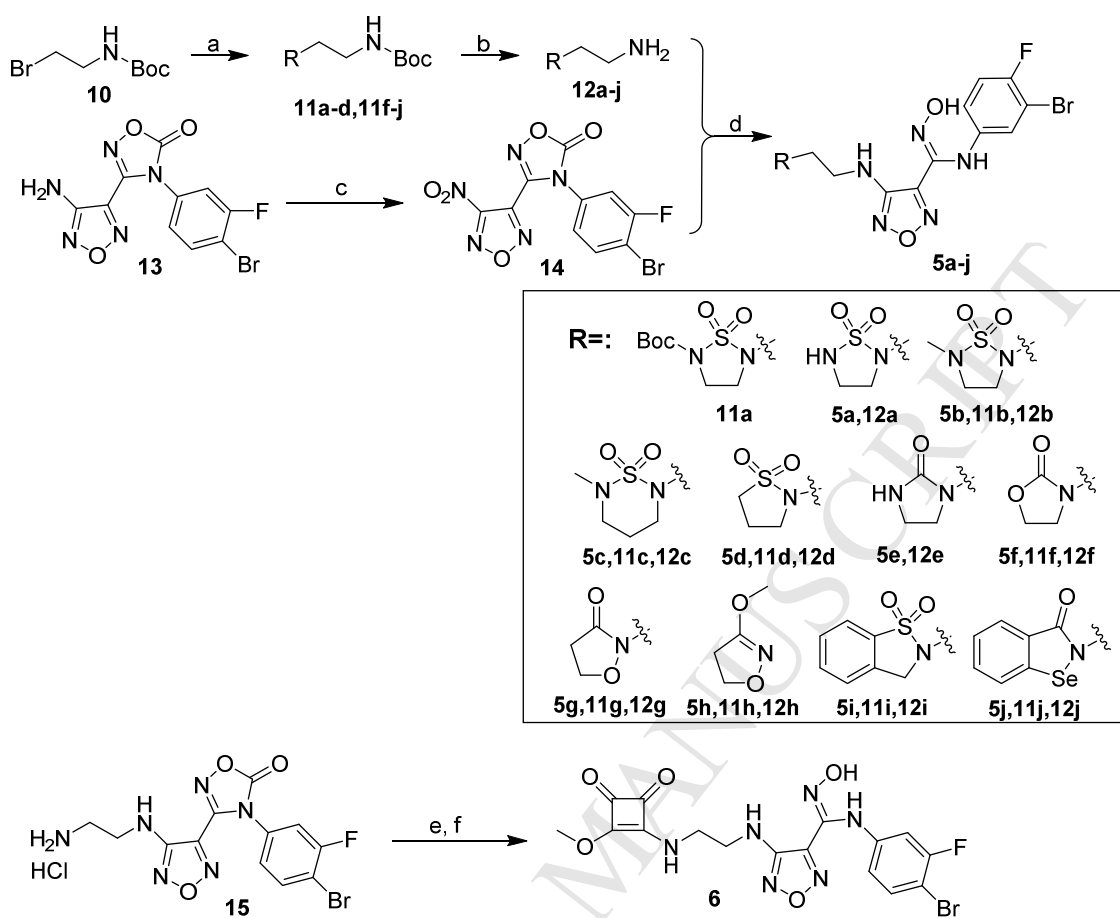


Figure 4. Survival curve. Mouse was euthanized when its tumor volume reached 3000 mm³ separately.

3. Chemistry

The procedures to synthesize all new compounds were outlined in Schemes 1-4. First, commercially available 2-(Boc-amino)ethyl bromide (**10**) was used as the starting material and reacted with different cyclic fragments in the presence of cesium carbonate to afford **11a-e** and **11g-j** in 76-84% yields, respectively (Scheme 1). Bromide **10** was reacted with 3-isoxazolidinone to afford two isomers **11g** and **11h**. Removal of the Boc-protecting group in **11a-d** and **11f-j** with trifluoroacetic acid (TFA) delivered the corresponding amines **12a-d** and **12f-j**. Oxidation of the key intermediate **13**⁶ with hydrogen peroxide and TFA gave intermediate **14** in 52% yield. Treatment of amines **12a-j** with **14** in the presence of 2.5 N NaOH produced target compounds **5a-j** in 25-30% overall yields (two steps). In addition, treatment of **15**⁶ with 3, 4-dimethoxy-3-cyclobutene-1,2-dione followed by deprotection with 2.5 N NaOH solution afforded the final product **6** in 22% overall yield.

Scheme 1.

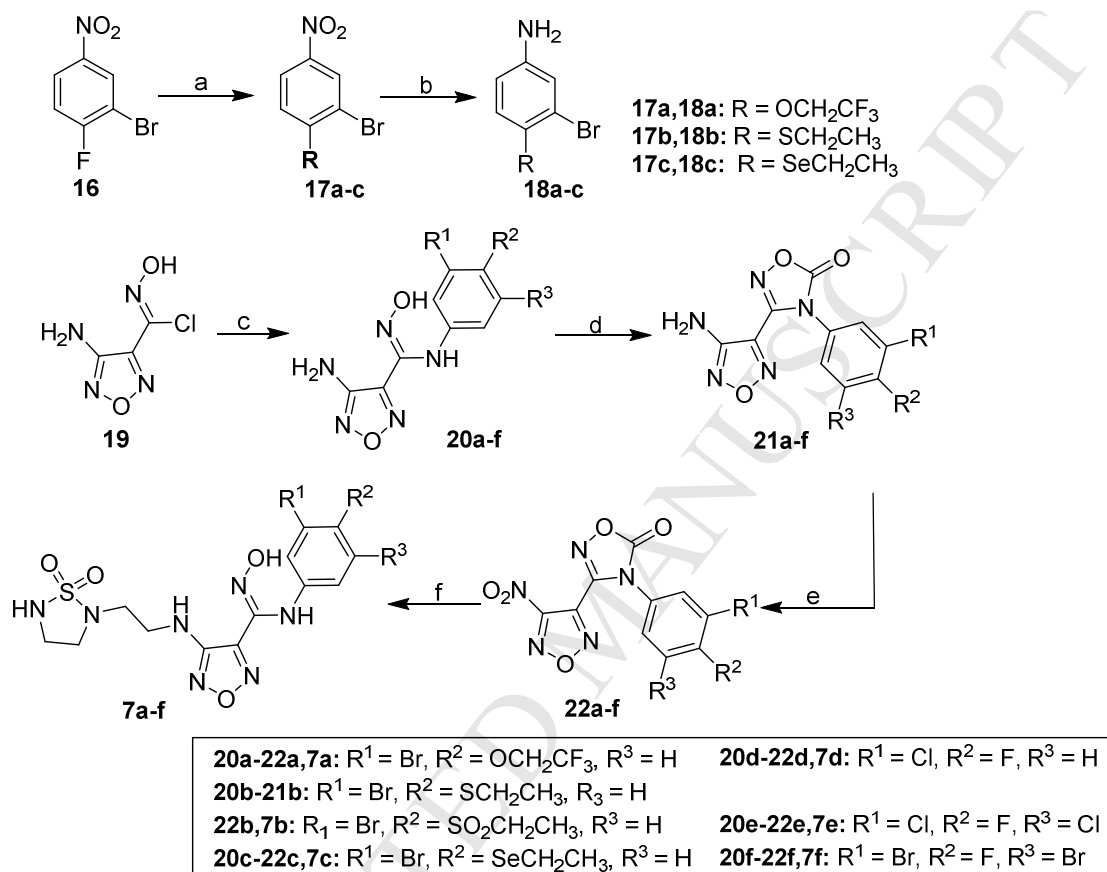


^aReagents and Conditions: (a) RH, Cs₂CO₃, DMF, rt, 76-84%; (b) CF₃COOH, DCM, rt, quantitative; (c) CF₃COOH, 30% H₂O₂, 45 °C, 52%; (d) 2.5 M NaOH, rt, 25-30%; (e) 3,4-dimethoxy-3-cyclobutene-1,2-dione, DIPEA, DMF; (f) 2.5 M NaOH, rt, 22% (two steps).

The synthesis of compounds **7a-f** was described in Scheme 2. Substitution of fluorobenzene **16** with different nucleophiles afforded nitrobenzenes **17a-c** in 72-91% yields. Reduction of **17a-c** with iron powder and ammonium chloride yielded anilines **18a-c** in 74-88% yields. Condensation of **19**³⁸ with differently substituted anilines delivered oxime derivatives **20a-f** in 68-80% yields. Protection of oxime derivatives **20a-f** in the presence of CDI provided 1,2,4-oxadiazol-5(4H)-ones **21a-f** in 98% yields. Oxidation of **21a-f** with hydrogen peroxide and TFA was found sluggish and yielded nitro compounds **22a-f** in 15-28% yields. It has to be mentioned that sulfane

21b was oxidized to sulfone **22b** during the reaction process. Amine **12a** was reacted with **22a-f** in the presence of 2.5 N NaOH solution to afford target compounds **7a-f** in 25-30% overall yields.

Scheme 2.

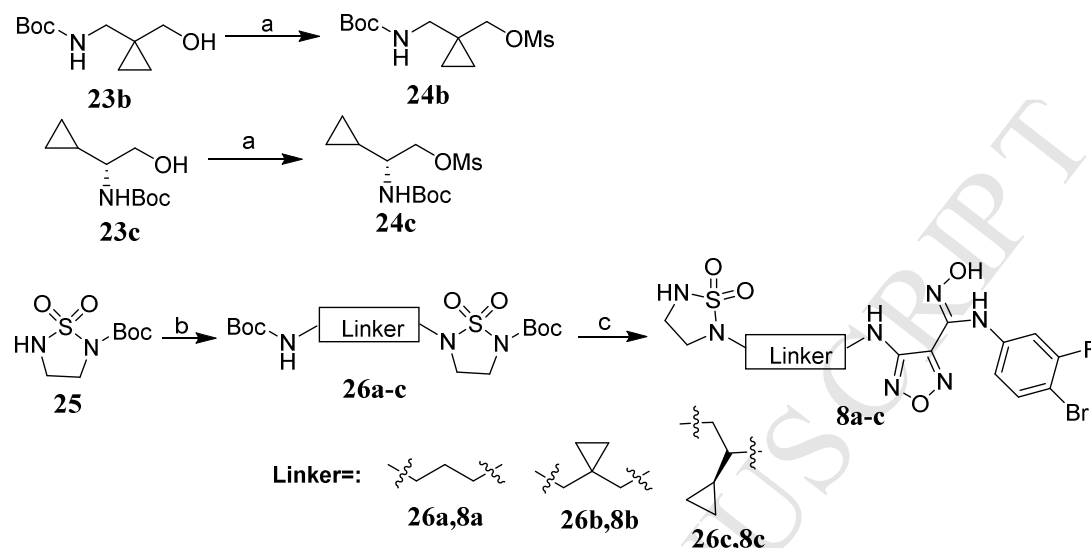


^aReagents and Conditions: (a) nucleophile, base, DMF, rt, 72-91%; (b) Fe, NH₄Cl, EtOH, reflux, 74-88%; (c) different aromatic amine analogue, NaHCO₃, EtOH, H₂O, 60 °C, 68-80%; (d) CDI, THF, reflux, ~98%; (e) CF₃COOH, 30% H₂O₂, 45 °C, 15-28%; (f) **12a**, 2.5 M NaOH, rt, 25-30%.

As shown in Scheme 3, substitution of alcohols **23b-c**³⁹⁻⁴⁰ with methanesulfonyl chloride (MsCl) generated **24b-c** in 65-72% yields. Reaction of *tert*-butyl 1,2,5-thiadiazolidine-2-carboxylate 1,1-dioxide (**25**)⁴¹ with different linkers led to compounds **26a-c** in 32-72% yields. After *N*-deprotection with TFA of **26a-c**, subsequent reaction with the intermediate **14** in the presence of 2.5 N NaOH solution

afforded the final compounds **8a-8c** in 21-33% overall yields (two steps).

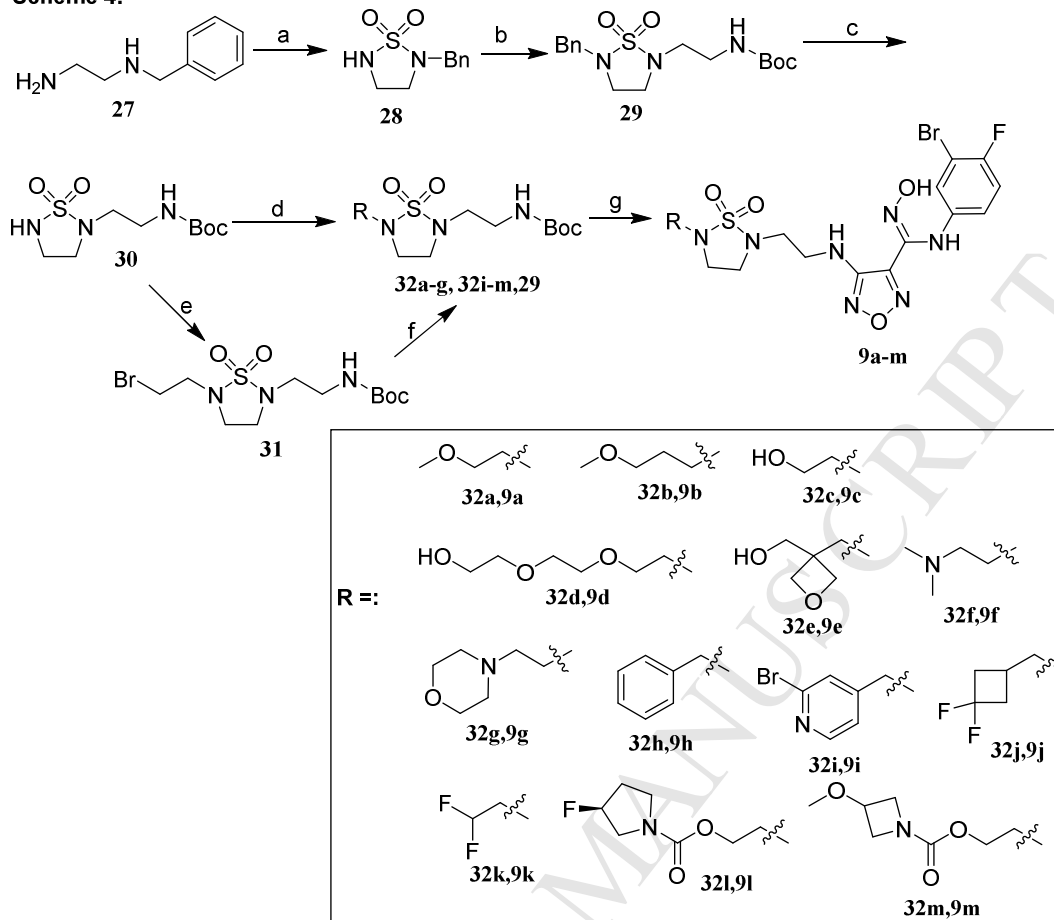
Scheme 3.



^aReagents and Conditions: (a) MsCl, Et₃N, DCM, rt, 65-72%; (b) **24b**, **24c** or *tert*-butyl 3-bromopropyl-carbamate, Cs₂CO₃, DMF, rt, 32-72%; (c) (i) CF₃COOH, DCM, rt, quantitative; (ii) **14**, 2.5 M NaOH, rt, 21-33%.

As shown in Scheme 4, *N*-benzylethane-1,2-diamine (**27**) was refluxed with sulfamide in pyridine to provide heterocycle **28** in 72% yield. Substitution of **28** with *tert*-butyl *N*-(2-bromoethyl)carbamate delivered the aminoethyl compound **29** in 75% yield. Removal of the benzyl group in **29** through catalytic hydrogenation afforded the key intermediate **30** in 87% yield. Compounds **32a-g** and **32i-k** were prepared from **30** via substitution reaction in the presence of cesium carbonate in 37-51% yields, respectively. Substitution of **30** with 1,2-dibromoethane resulted in the intermediate **31** in 45% yield. Compounds **32l** and **32m** were synthesized by nucleophilic displacement from bromide **31** in the presence of cesium carbonate in 37% and 51% yields, respectively. Removal of the *N*-Boc protective group in **32a-g**, **29** and **32i-m** with TFA followed by reaction with the intermediate **14** in the presence of 2.5 N NaOH solution afforded target compounds **9a-m** in 16-43% overall yields (two steps).

Scheme 4.



^aReagents and Conditions: (a) sulfamide, pyridine, reflux, 72 %; (b) **10**, Cs₂CO₃, DMF, rt, 75 %; (c) Pd(OH)₂, 50 °C, MeOH, 87%; (d) RBr, Cs₂CO₃, DMF, rt, 42-78%; (e) 1,2-dibromoethane, Cs₂CO₃, DMF, rt, 45%; (f) (R)-(-)-3-fluoropyrrolidine hydrochloride or 3-methoxy-azetidine, Cs₂CO₃, DMF, rt, 37-51 %; (g) (i) CF₃COOH, DCM, rt, quantitative; (ii) **14**, 2.5 M NaOH, rt, 16-43%.

4. Conclusion

PD-1/PD-L1, CTLA-4, and IDO1 are the frontier oncology immuno-therapeutic targets. However, unlike the cell-surface checkpoint receptor molecules that can be effectively targeted by antibody-based inhibitors, IDO1 or its downstream effectors are intracellular targets that are ideally targeted by small molecules. Epacadostat is the most advanced IDO1 inhibitor, but its clinical trial as monotherapy is unsuccessful. Recent failure of its combination with PD-1 antibody blockade in phase III trial in melanoma further deterred many other clinical trials with IDO1 inhibitors. To gain

more insight on the antitumor efficacy of IDO1 inhibitors, we have designed a series of analogues of epacadostat by incorporating a cyclic aminosulfonamide moiety as the sidechain capping functionality. Subsequent multidimensional optimization of the heterocyclic skeleton, *N*-substituent as well as the linker led to identification of compound **5a** showing good potency compatible to that of epacadostat against hIDO1 and IDO1-expressing HEK293 cells. This compound has improved physico-chemical properties, acceptable PK parameters as well as optimal cardiac safety. Furthermore, in the CT-26 syngeneic xenograft model, treatment with our new IDO1 inhibitor **5a** or the clinical drug epacadostat produced marginal antitumor activity in 14 d - treatment regimen, which is not statistically different from that of the vehicle group. However, the combination of **5a** with PD-1 antibody produced elevated antitumor activity. Moreover, the life span of mice was also significantly extended in the combination treatment group. Combining the outcomes of epacadostat and our only inhibitor **5a**, it might be more reasonable to pursue the overall benefits of IDO1 inhibitors in a much broader vision rather than only focusing on antitumor efficacy, for example, the median survival time of tumor patients.

5. Experimental

5.1. Chemistry.

5.1.1. General methods

All reactions were performed in glassware containing a Teflon coated stir bar. Commercial solvents and reagents were obtained from sources Adamas-beta, Acros

Organics, Bidepharm, Alfa Aesar, J&K, TCI, and Accela and used without further purification. ^1H and ^{13}C NMR spectra were recorded with a Varian-MERCURY Plus 300, 400 or 500 MHz NMR spectrometer and referenced to deuterium dimethyl sulfoxide (DMSO-d_6), deuterium acetonitrile (CD_3CN), deuterium chloroform (CDCl_3). Chemical shifts (δ) were reported in ppm downfield from an internal TMS standard. Low- and high-resolution mass spectra were obtained in the ESI mode. Flash column chromatography on silica gel (200–300 mesh) was used for the routine purification of reaction products. The column outputs were monitored by TLC on silica gel (200–300 mesh) precoated on glass plates (15 mm \times 50 mm), and spots were visualized by UV light at 254 or 365 nm. Some outputs were colored by basic KMnO_4 solution or ninhydrin reagent. HPLC analysis was conducted for all biologically evaluated compounds on an Agilent Technologies 1260 series LC system with ultraviolet wavelengths in UV 254 to determine the chemical purity and optical purity. The purities of all biologically evaluated compounds were above 95%.

5.1.2. Synthesis of new IDO inhibitors

N-(3-Bromo-4-fluorophenyl)-4-((2-(1,1-dioxido-1,2,5-thiadiazolidin-2-yl)ethyl)amino)-N'-hydroxy-1,2,5-oxadiazole-3-carboximidamide (5a). To the mixture of the precursor **10** (2.26 g, 10.1 mmol, 1.5 equiv) and *tert*-butyl 1,2,5-thiadiazolidine-2-carboxylate 1,1-dioxide (1.50 g, 6.75 mmol, 1.0 equiv) in dry DMF (10 mL), was added Cs_2CO_3 (6.60 g, 20.25 mmol, 3.0 equiv). The mixture was stirred at room temperature overnight, and then extracted with ethyl acetate. The organic phase was washed with saturated NaHCO_3 and brine, dried over anhydrous

Na₂SO₄, filtered and concentrated. The resulting residue was purified via silica gel chromatography to give **11a** as colorless oil (1.96 g, 79%). ¹H NMR (300 MHz, CDCl₃) δ 4.89 (br, 1H), 3.80 (t, *J* = 6.5 Hz, 2H), 3.47 – 3.34 (m, 4H), 3.18 (t, *J* = 6.1 Hz, 2H), 1.54 (s, 9H), 1.44 (s, 9H).

The obtained compound **11a** (730 mg, 2 mmol, 1.0 equiv) dissolved in DCM (5 mL). TFA (5 mL) was added and the mixture was stirred at room temperature until the starting material was consumed completely. The solvent was removed under vacuum to afford intermediate **12a**, which was employed for use without further purification.

To the mixture of **13** (2.0 g, 5.85 mmol, 1.0 equiv) and TFA (23 mL), was added 30% hydrogen peroxide solution (15 mL). The reaction mixture was heated at 45 °C for 2 days. Ethyl acetate (20 mL) and saturated NaS₂O₃ solution (50 mL) were added, and the mixture was allowed to stir for 20 min. Additional ethyl acetate was added and the reaction mixture was partitioned between ethyl acetate and water. The organic phase was washed with water and brine, then dried over anhydrous Na₂SO₄, filtered and concentrated. The resulting residue was further purified via silica gel chromatography to give **14** as a yellow solid (1.12 g, 52%). ¹H NMR (400 MHz, CDCl₃) δ 7.65 – 7.55 (m, 1H), 7.30 – 7.20 (m, 2H).

The intermediate **12a** (42 mg, 0.25 mmol, 1.0 equiv) and **14** (93 mg, 0.25 mmol, 1.0 equiv) were dissolved in THF (5 mL). 2.5 N NaOH solution (0.5 mL) was added and the mixture was stirred at room temperature for 3 h. After extraction with ethyl acetate, the combined organic phase was washed with water and brine, dried over anhydrous Na₂SO₄, filtered and then concentrated. The resulting residue was purified

via silica gel chromatography to give target compound **5a** as white solid (29 mg, 25%). ¹H NMR (400 MHz, CD₃CN) δ 9.08 (s, 1H), 7.51 (s, 1H), 7.25 (dd, *J* = 6.0, 2.5 Hz, 1H), 7.12 (t, *J* = 8.7 Hz, 1H), 6.99 – 6.92 (m, 1H), 6.07 (t, *J* = 7.6 Hz, 1H), 5.21 (s, 1H), 3.54 (dd, *J* = 12.3, 6.2 Hz, 2H), 3.44 (dt, *J* = 11.5, 6.0 Hz, 4H), 3.25 (t, *J* = 6.1 Hz, 2H). ¹³C NMR (126 MHz, CD₃CN) δ 156.80, 156.57 (d, *J* = 241.9 Hz), 142.26, 140.18, 138.16 (d, *J* = 3.8 Hz), 128.51, 124.81 (d, *J* = 7.6 Hz), 116.87 (d, *J* = 22.7 Hz), 108.43 (d, *J* = 21.4 Hz), 50.48, 46.17, 43.33, 40.80. ESI-MS: *m/z* 462.3 [M-H]⁻; HRMS-ESI: *m/z* [M-H]⁻ calcd for C₁₃H₁₄BrFN₇O₄S: 462.0001, found: 462.0006.

Compounds **5b-j** were synthesized according to a similar protocol as that described for **5a**.

N-(3-Bromo-4-fluorophenyl)-N'-hydroxy-4-((2-(5-methyl-1,1-dioxido-1,2,5-thiadiazolidin-2-yl)ethyl)amino)-1,2,5-oxadiazole-3-carboximidamide (5b). Yellow foam (30%). ¹H NMR (400 MHz, CD₃CN) δ 9.14 (s, 1H), 7.48 (s, 1H), 7.21 (dd, *J* = 6.0, 2.7 Hz, 1H), 7.08 (t, *J* = 8.7 Hz, 1H), 7.02 – 6.88 (m, 1H), 6.03 (t, *J* = 6.0 Hz, 1H), 3.50 (q, *J* = 6.1 Hz, 2H), 3.41 – 3.34 (m, 2H), 3.29 – 3.23 (m, 4H), 2.65 (s, 3H). ¹³C NMR (126 MHz, CD₃CN) δ 155.86, 155.62 (d, *J* = 241.9 Hz), 141.31, 139.26, 137.23 (d, *J* = 2.5 Hz), 127.54, 123.83 (d, *J* = 6.3 Hz), 115.93 (d, *J* = 23.9 Hz), 107.49 (d, *J* = 22.7 Hz), 47.46, 46.17, 45.78, 42.20, 33.29. ESI-MS: *m/z* 476.4 [M-H]⁻; HRMS-ESI: *m/z* [M-H]⁻ calcd for C₁₄H₁₆BrFN₇O₄S: 476.0157, found: 476.0165.

N-(3-Bromo-4-fluorophenyl)-N'-hydroxy-4-((2-(6-methyl-1,1-dioxido-1,2,6-thiadiazinan-2-yl)ethyl)amino)-1,2,5-oxadiazole-3-carboximidamide (5c). Colorless foam (28%). ¹H NMR (400 MHz, CD₃CN) δ 9.12 (s, 1H), 7.51 (s, 1H), 7.24 (dd, *J* =

6.1, 2.7 Hz, 1H), 7.12 (t, $J = 8.7$ Hz, 1H), 6.95 (m, 1H), 6.03 (t, $J = 7.9$ Hz, 1H), 3.46 (m, 4H), 3.40 – 3.26 (m, 4H), 2.73 (s, 3H), 1.89 – 1.75 (m, 2H). ^{13}C NMR (126 MHz, CD_3CN) δ 156.85, 156.59 (d, $J = 243.2$ Hz), 142.37, 140.23, 138.22 (d, $J = 2.5$ Hz), 128.51, 124.79 (d, $J = 7.6$ Hz), 116.90 (d, $J = 23.9$ Hz), 108.45 (d, $J = 22.7$ Hz), 53.27, 51.17, 47.87, 43.49, 37.11, 20.01. ESI-MS: m/z 490.4 $[\text{M}-\text{H}]^-$; HRMS-ESI: m/z $[\text{M}-\text{H}]^-$ calcd for $\text{C}_{15}\text{H}_{18}\text{BrFN}_7\text{O}_4\text{S}$: 490.0314, found: 490.0316.

N-(3-Bromo-4-fluorophenyl)-4-((2-(1,1-dioxidoisothiazolidin-2-yl)ethyl)amino)-N'-hydroxy-1,2,5-oxadiazole-3-carboximidamide (5d). White solid (28%). ^1H NMR (400 MHz, CD_3CN) δ 9.22 (s, 1H), 7.52 (s, 1H), 7.24 (dd, $J = 6.0, 2.7$ Hz, 1H), 7.11 (t, $J = 8.7$ Hz, 1H), 7.01 – 6.89 (m, 1H), 6.05 (t, $J = 5.7$ Hz, 1H), 3.50 (q, $J = 6.0$ Hz, 2H), 3.33 (t, $J = 6.7$ Hz, 2H), 3.25 (t, $J = 6.0$ Hz, 2H), 3.18 – 3.09 (m, 2H), 2.38 – 2.29 (m, 2H). ^{13}C NMR (126 MHz, CD_3CN) δ 156.82, 156.49 (d, $J = 241.9$ Hz), 142.18, 140.21, 138.20 (d, $J = 2.5$ Hz), 128.38, 124.67 (d, $J = 7.6$ Hz), 116.84 (d, $J = 23.9$ Hz), 108.40 (d, $J = 22.7$ Hz), 47.96, 47.26, 44.14, 43.06, 19.69. ESI-MS: m/z 461.4 $[\text{M}-\text{H}]^-$; HRMS-ESI: m/z $[\text{M}-\text{H}]^-$ calcd for $\text{C}_{14}\text{H}_{15}\text{BrFN}_6\text{O}_4\text{S}$: 461.0048, found: 461.0050.

N-(3-Bromo-4-fluorophenyl)-N'-hydroxy-4-((2-(2-oxoimidazolidin-1-yl)ethyl)amino)-1,2,5-oxadiazole-3-carboximidamide (5e). White solid (27%). ^1H NMR (400 MHz, CD_3CN) δ 10.07 (s, 1H), 7.50 (s, 1H), 7.23 (m, 1H), 7.11 (t, $J = 8.7$ Hz, 1H), 6.94 (m, 1H), 6.09 (s, 1H), 5.01 (s, 1H), 3.54 – 3.46 (m, 2H), 3.46 – 3.39 (m, 4H), 3.39 – 3.31 (m, 2H). ^{13}C NMR (126 MHz, CD_3CN) δ 164.41, 156.90, 156.36 (d, $J = 241.9$ Hz), 141.91, 140.14, 138.41, 128.15, 124.46 (d, $J = 7.6$ Hz), 116.79 (d, $J = 23.9$

Hz), 108.34 (d, $J = 11.3$ Hz), 45.77, 43.55, 43.15, 38.97. ESI-MS: m/z 426.5 [M-H]⁻; HRMS-ESI: m/z [M-H]⁻ calcd for C₁₄H₁₄BrFN₇O₃S: 426.0331, found: 426.0335.

N-(3-Bromo-4-fluorophenyl)-N'-hydroxy-4-((2-(2-oxooxazolidin-3yl)ethyl)amino)-1,2,5-oxadiazole-3-carboximidamide (5f). Faint yellow solid (25%). ¹H NMR (400 MHz, CD₃CN) δ 9.46 (s, 1H), 7.52 (s, 1H), 7.24 (dd, $J = 6.0, 2.7$ Hz, 1H), 7.11 (t, $J = 8.7$ Hz, 1H), 6.94 (m, 1H), 6.04 (s, 1H), 4.37 – 4.22 (m, 2H), 3.71 – 3.59 (m, 2H), 3.50 (dd, $J = 8.5, 1.8$ Hz, 4H). ¹³C NMR (126 MHz, CD₃CN) δ 160.16, 156.89, 156.46 (d, $J = 241.9$ Hz), 142.09, 140.16, 138.23, 128.30, 124.62 (d, $J = 6.3$ Hz), 116.83 (d, $J = 23.9$ Hz), 108.39 (d, $J = 22.7$ Hz), 63.23, 45.41, 43.67, 42.85. ESI-MS: m/z 427.4 [M-H]⁻; HRMS-ESI: m/z [M-H]⁻ calcd for C₁₄H₁₃BrFN₆O₄S: 427.0171, found: 427.0196.

N-(3-Bromo-4-fluorophenyl)-N'-hydroxy-4-((2-(3-oxoisoxazolidin-2-yl)ethyl)amino)-1,2,5-oxadiazole-3-carboximidamide (5g). White solid (28%). ¹H NMR (400 MHz, CD₃CN) δ 9.16 (s, 1H), 7.49 (s, 1H), 7.23 (dd, $J = 6.1, 2.7$ Hz, 1H), 7.10 (t, $J = 8.7$ Hz, 1H), 6.93 (m, 1H), 6.03 (s, 1H), 4.32 (t, $J = 8.1$ Hz, 2H), 3.72 (t, $J = 5.7$ Hz, 2H), 3.51 (dd, $J = 11.8, 5.9$ Hz, 2H), 2.70 (t, $J = 8.0$ Hz, 2H). ¹³C NMR (126 MHz, CD₃CN) δ 164.41, 156.90, 156.36 (d, $J = 241.9$ Hz), 141.91, 140.14, 138.41, 128.15, 124.46 (d, $J = 7.6$ Hz), 116.79 (d, $J = 23.9$ Hz), 108.34 (d, $J = 11.3$ Hz), 45.77, 43.55, 43.15, 38.97. ESI-MS: m/z 427.4 [M-H]⁻; HRMS-ESI: m/z [M-H]⁻: calcd for C₁₄H₁₃BrFN₆O₄S: 427.0171, found: 427.0169.

N-(3-Bromo-4-fluorophenyl)-4-((2-((4,5-dihydroisoxazol-3-yl)oxy)ethyl)amino)-N'-hydroxy-1,2,5-oxadiazole-3-carboximidamide (5h). White solid (28%). ¹H

NMR (400 MHz, CD₃CN) δ 9.11 (s, 1H), 7.52 (s, 1H), 7.25 (dd, J = 6.0, 2.7 Hz, 1H), 7.12 (t, J = 8.7 Hz, 1H), 6.96 (m, 1H), 6.14 (t, J = 5.6 Hz, 1H), 4.42 – 4.27 (m, 4H), 3.64 (dd, J = 10.9, 5.7 Hz, 2H), 2.99 (t, J = 9.6 Hz, 2H). ¹³C NMR (126 MHz, CD₃CN) δ 168.96, 156.88, 156.64 (d, J = 243.2 Hz), 142.29, 140.20, 138.14 (d, J = 3.8 Hz), 128.61, 124.88 (d, J = 7.6 Hz), 116.89 (d, J = 23.9 Hz), 108.43 (d, J = 22.7 Hz), 70.41, 68.76, 44.10, 33.66. ESI-MS: m/z 427.3 [M-H]⁻; HRMS-ESI: m/z [M-H]⁻ calcd for C₁₄H₁₃BrFN₆O₄S: 427.0171, found: 427.0176.

N-(3-Bromo-4-fluorophenyl)-4-((2-(1,1-dioxidobenzo[d]isothiazol-2(3H)-yl)ethylamino)-N'-hydroxy-1,2,5-oxadiazole-3-carboximidamide (5i). Faint yellow solid (28%). ¹H NMR (400 MHz, CD₃CN) δ 8.99 (s, 1H), 7.81 (d, J = 7.4 Hz, 1H), 7.72 (m, 1H), 7.65 – 7.54 (m, 2H), 7.49 (s, 1H), 7.23 (dd, J = 6.1, 2.8 Hz, 1H), 7.08 (t, J = 8.7 Hz, 1H), 6.97 – 6.90 (m, 1H), 6.12 (t, J = 6.0 Hz, 1H), 4.55 (s, 2H), 3.66 (q, J = 5.9 Hz, 2H), 3.55 (t, J = 5.7 Hz, 2H). ¹³C NMR (126 MHz, CD₃CN) δ 156.86, 156.56 (d, J = 241.9 Hz), 142.26, 140.27, 138.19 (d, J = 3.8 Hz), 135.77, 135.21, 133.90, 130.22, 128.48, 126.11, 124.76 (d, J = 6.3 Hz), 121.69, 116.86 (d, J = 22.7 Hz), 108.45 (d, J = 22.7 Hz), 51.57, 43.30, 43.12. ESI-MS: m/z 509.4 [M-H]⁻; HRMS-ESI: m/z [M-H]⁻ calcd for C₁₈H₁₅BrFN₆O₄S: 509.0048, found: 509.0046.

N-(3-Bromo-4-fluorophenyl)-N'-hydroxy-4-((2-(3-oxobenzo[d][1,2]selenazol-2(3H)-yl)ethylamino)-1,2,5-oxadiazole-3-carboximidamide (5j). White solid (25%). ¹H NMR (400 MHz, MeOD) δ 7.98 – 7.87 (m, 2H), 7.65 – 7.59 (m, 1H), 7.45 (t, J = 7.5 Hz, 1H), 7.12 (dd, J = 6.0, 2.7 Hz, 1H), 7.02 (t, J = 8.7 Hz, 1H), 6.81 (m, 1H), 4.16 – 4.06 (m, 2H), 3.70 – 3.61 (m, 2H). ¹³C NMR (126 MHz, MeOD) δ 169.79,

156.95, 156.62 (d, $J = 241.9$ Hz), 141.96, 141.49, 140.84, 139.11 (d, $J = 2.5$ Hz), 133.11, 128.83, 128.60, 127.78, 127.17, 126.29, 123.87 (d, $J = 7.6$ Hz), 116.68 (d, $J = 23.9$ Hz), 108.76 (d, $J = 21.4$ Hz), 45.29, 43.88. ESI-MS: m/z 539.3 [M-H]⁻; HRMS-ESI: m/z [M-H]⁻ calcd for C₁₈H₁₃BrFN₆O₃Se: 538.9387, found: 538.9382.

N-(4-Bromo-3-fluorophenyl)-N'-hydroxy-4-((2-((2-methoxy-3,4-dioxocyclobut-1-en-1-yl)amino)ethyl)amino)-1,2,5-oxadiazole-3-carboximidamide (6). To the mixture of **15** (100 mg, 0.24 mmol, 1.0 equiv) and 3,4-dimethoxy-3-cyclobutene-1,2-dione (41 mg, 0.29 mmol, 1.2 equiv) in dry DMF (1 mL), was added DIPEA (62 mg, 0.48 mmol, 2.0 equiv). The mixture was stirred at room temperature overnight and then extracted with ethyl acetate. The combined organic phase was washed with water and brine, dried over anhydrous Na₂SO₄, filtered and concentrated. The resulting residue was dissolved in THF and was added 2.5 N NaOH solution (1 mL). After stirring at room temperature for 3 h, the mixture was diluted with ethyl acetate and water. The organic phase was washed with water and brine, dried over anhydrous Na₂SO₄, filtered and concentrated. The resulting residue was purified via silica gel chromatography to give **6** as a white solid (25 mg, 22%). ¹H NMR (400 MHz, CD₃OD) δ 9.19 (s, 1H), 7.50 (s, 1H), 7.22 (dd, $J = 5.5, 1.6$ Hz, 1H), 7.10 (t, $J = 8.7$ Hz, 1H), 6.92 (m, 1H), 6.76 (d, $J = 55.1$ Hz, 1H), 6.10 (s, 1H), 4.35-4.31 (m, 3H), 3.82 – 3.42 (m, 4H). ¹³C NMR (126 MHz, CD₃CN) δ 190.13, 173.99, 157.56 (d, $J = 241.9$ Hz), 156.75, 142.19, 140.27, 138.14 (d, $J = 2.5$ Hz), 128.55, 124.82 (d, $J = 7.6$ Hz), 116.88 (d, $J = 22.7$ Hz), 108.44 (d, $J = 22.7$ Hz), 60.99, 45.65, 45.35, 43.64, 30.30. ESI-MS: m/z 467.4 [M-H]⁻; HRMS-ESI: m/z [M-H]⁻ calcd

for $C_{16}H_{13}BrFN_6O_5$: 467.0012, found: 467.0016.

N-(3-Bromo-4-(2,2,2-trifluoroethoxy)phenyl)-4-((2-(1,1-dioxido-1,2,5-thiadiazolidin-2-yl)ethyl)amino)-N'-hydroxy-1,2,5-oxadiazole-3-carboximidamide (7a).

2-Bromo-1-fluoro-4-nitrobenzene (1.0 g, 4.55 mmol, 1.0 equiv) in THF (5 mL) was added to a mixture of 2,2,2-trifluoro-ethanol (0.5 g, 5 mmol, 1.1 equiv) and potassium *tert*-butylate (764 mg, 6.82 mmol, 1.5 equiv.) in THF (10 mL) at 5 °C. The mixture was stirred for 5 h at 5 °C, and then quenched by pouring into water. The aqueous phase was extracted with ethyl acetate and washed with water and brine. The combined organic phase was dried over anhydrous Na_2SO_4 , filtered and concentrated. The resulting residue was purified via silica gel chromatography to give **17a** (1.24 g, 91%) as a brown oil. 1H NMR (300 MHz, $CDCl_3$) δ 8.51 (d, $J = 2.7$ Hz, 1H), 8.23 (dd, $J = 9.1, 2.7$ Hz, 1H), 6.98 (d, $J = 9.1$ Hz, 1H), 4.52 (q, $J = 7.7$ Hz, 2H).

To the mixture of **17a** (600 mg, 2.0 mmol, 1.0 equiv) and iron powder (336 mg, 6.0 mmol, 3.0 equiv) in ethanol (10 mL), was added ammonium chloride solution (10 mmol, 5.0 equiv). The mixture was stirred at reflux for 6 h, and then cooled to 25 °C. After diluted with ethyl acetate, the organic phase was washed with water and brine. The organic layer was separated, dried over anhydrous Na_2SO_4 , filtered and concentrated. The resulting residue was purified via silica gel chromatography to give **18a** (475 mg, 88%). 1H NMR (400 MHz, $CDCl_3$) δ 6.92 (d, $J = 2.8$ Hz, 1H), 6.87 (d, $J = 8.7$ Hz, 1H), 6.60 (dd, $J = 8.7, 2.8$ Hz, 1H), 4.32 (q, $J = 8.3$ Hz, 2H), 3.61 (br, 2H).

To a mixture of compound **19** (211 mg, 1.3 mmol, 1.0equiv) in ethanol (10 mL) at 60 °C, **18a** (351 mg, 1.3 mmol, 1.0 equiv) was added. The reaction was stirred for

10 min, and then a warm sodium bicarbonate solution (328 mg in 5 mL water) was added over 15 min. The reaction was stirred at 60 °C for 1 h and then cooled to room temperature. After extraction with ethyl acetate, the combined organic phase was dried over sodium sulfate and concentrated to give **20a** as a crude brown solid (515 mg, 80%). ¹H NMR (300 MHz, DMSO) δ 11.29 (s, 1H), 8.73 (s, 1H), 7.08 (dd, *J* = 16.2, 5.7 Hz, 2H), 6.75 (dd, *J* = 8.9, 2.7 Hz, 1H), 6.24 (s, 2H), 4.75 (q, *J* = 8.9 Hz, 2H).

A mixture of **20a** (396 mg, 1.0 mmol, 1.0 equiv) and CDI (195 mg, 1.2 mmol, 1.2 equiv) in THF (10 mL) was heated to reflux and stirred for 2 h. After cooled to room temperature, the mixture was extracted with DCM. The organic phase was washed with 1N HCl and brine, dried over sodium sulfate, and then concentrated to give the desired product **21a** (413 mg, 98%) as a crude brown solid. ¹H NMR (300 MHz, DMSO) δ 7.97 (d, *J* = 2.4 Hz, 1H), 7.64 (dd, *J* = 8.9, 2.5 Hz, 1H), 7.37 (d, *J* = 9.0 Hz, 1H), 6.59 (s, 2H), 4.96 (q, *J* = 8.6 Hz, 2H).

Compound **22a** was obtained from **21a** according to a similar procedure as that for **14**. Yellow solid (28%); ¹H NMR (400 MHz, CDCl₃) δ 7.60 (d, *J* = 2.6 Hz, 1H), 7.29 (dd, *J* = 8.8, 2.7 Hz, 1H), 7.01 (d, *J* = 8.8 Hz, 1H), 4.47 (q, *J* = 7.8 Hz, 2H).

Compound **7a** was obtained from **22a** and **12a** according to a similar procedure as that for **5a**. White solid (25%). ¹H NMR (400 MHz, CD₃CN) δ 9.15 (s, 1H), 7.45 (s, 1H), 7.24 (s, 1H), 7.04 – 6.85 (m, 2H), 6.05 (t, *J* = 5.8 Hz, 1H), 5.23 (s, 1H), 4.54 (q, *J* = 8.5 Hz, 2H), 3.50 (q, *J* = 6.1 Hz, 2H), 3.45 – 3.34 (m, 4H), 3.21 (t, *J* = 6.1 Hz, 2H). ¹³C NMR (126 MHz, CD₃CN) δ 157.01, 151.69, 142.74, 140.34, 136.72, 129.42,

124.88, 115.67, 112.17, 67.81 (q, $J = 35.3$ Hz), 50.62, 46.33, 43.48, 40.98. ESI-MS: m/z 542.4 [M-H]⁻; HRMS-ESI: m/z [M-H]⁻ calcd for C₁₅H₁₆BrF₃N₇O₅S: 542.0075, found: 542.0079.

Compounds **7b-f** were prepared according to a similar protocol as that described for **7a**.

N-(3-Bromo-4-(ethylsulfonyl)phenyl)-4-((2-(1,1-dioxido-1,2,5-thiadiazolidin-2-yl)ethyl)amino)-N'-hydroxy-1,2,5-oxadiazole-3-carboximidamide (7b). White solid (29%). ¹H NMR (400 MHz, CD₃CN) δ 9.59 (s, 1H), 7.88 (d, $J = 8.7$ Hz, 1H), 7.77 (s, 1H), 7.23 (d, $J = 2.2$ Hz, 1H), 6.94 (dd, $J = 8.6, 2.2$ Hz, 1H), 6.00 (s, 1H), 5.21 (s, 1H), 3.53 (q, $J = 6.1$ Hz, 2H), 3.47 – 3.32 (m, 6H), 3.24 (t, $J = 6.1$ Hz, 2H), 1.16 (t, $J = 7.4$ Hz, 3H). ¹³C NMR (151 MHz, CD₃CN) δ 156.55, 146.76, 140.78, 140.11, 133.24, 130.76, 126.04, 121.20, 118.86, 50.41, 49.22, 46.08, 43.28, 40.76, 7.44. ESI-MS: m/z 536.4 [M-H]⁻; HRMS-ESI: m/z [M-H]⁻ calcd for C₁₅H₁₉BrN₇O₆S₂: 536.0027, found: 536.0024.

N-(3-Bromo-4-(ethylselanyl)phenyl)-4-((2-(1,1-dioxido-1,2,5-thiadiazolidin-2-yl)ethyl)amino)-N'-hydroxy-1,2,5-oxadiazole-3-carboximidamide (7c). White solid (30%). ¹H NMR (400 MHz, CD₃CN) δ 9.16 (s, 1H), 7.51 (s, 1H), 7.28 (d, $J = 8.5$ Hz, 1H), 7.19 (d, $J = 2.4$ Hz, 1H), 6.88 (dd, $J = 8.5, 2.4$ Hz, 1H), 6.05 (t, $J = 5.9$ Hz, 1H), 5.23 (t, $J = 5.7$ Hz, 1H), 3.53 (q, $J = 6.1$ Hz, 2H), 3.48 – 3.38 (m, 4H), 3.25 (t, $J = 6.1$ Hz, 2H), 2.98 (q, $J = 7.5$ Hz, 2H), 1.45 (t, $J = 7.4$ Hz, 3H). ¹³C NMR (126 MHz, CD₃CN) δ 156.80, 141.96, 140.31, 140.15, 131.52, 128.35, 127.38, 125.11, 123.26, 50.48, 46.18, 43.36, 40.81, 21.41, 14.97. ESI-MS: m/z 552.3 [M-H]⁻;

HRMS-ESI: m/z [M-H]⁻ calcd for C₁₅H₁₉BrN₇O₄SSe: 551.9573, found: 551.9584.

N-(3-Chloro-4-fluorophenyl)-4-((2-(1,1-dioxido-1,2,5-thiadiazolidin-2-yl)ethyl)amino)-N'-hydroxy-1,2,5-oxadiazole-3-carboximidamide (7d). Colorless foam (25%). ¹H NMR (400 MHz, CD₃CN) δ 9.13 (s, 1H), 7.51 (s, 1H), 7.14 (t, J = 9.0 Hz, 1H), 7.10 (dd, J = 6.6, 2.8 Hz, 1H), 6.91 (m, 1H), 6.08 (t, J = 5.5 Hz, 1H), 5.24 (s, 1H), 3.53 (q, J = 6.1 Hz, 2H), 3.49 – 3.35 (m, 4H), 3.25 (t, J = 6.1 Hz, 2H). ¹³C NMR (126 MHz, CD₃CN) δ 156.81, 155.53 (d, J = 243.2 Hz), 142.26, 140.21, 137.94 (d, J = 3.8 Hz), 125.66, 124.02 (d, J = 7.6 Hz), 120.60 (d, J = 8.9 Hz), 117.10 (d, J = 22.7 Hz), 50.48, 46.18, 43.34, 40.81. ESI-MS: m/z 418.3 [M-H]⁻; HRMS-ESI: m/z [M-H]⁻ calcd for C₁₃H₁₄ClFN₇O₄S: 418.0506, found: 418.0502.

N-(3,5-Dichloro-4-fluorophenyl)-4-((2-(1,1-dioxido-1,2,5-thiadiazolidin-2-yl)ethyl)amino)-N'-hydroxy-1,2,5-oxadiazole-3-carboximidamide (7e). White solid (25%). ¹H NMR (400 MHz, CD₃CN) δ 9.20 (s, 1H), 7.50 (s, 1H), 7.00 (d, J = 5.9 Hz, 2H), 6.04 (t, J = 4.9 Hz, 1H), 5.18 (s, 1H), 3.51 (q, J = 6.1 Hz, 2H), 3.46 – 3.34 (m, 4H), 3.22 (t, J = 6.1 Hz, 2H). ¹³C NMR (126 MHz, CD₃CN) δ 156.78, 151.31 (d, J = 244.4 Hz), 141.60, 140.26, 138.01 (d, J = 3.8 Hz), 123.70 (2C), 122.09, 121.94, 50.53, 46.19, 43.38, 40.83. ESI-MS: m/z 452.3 [M-H]⁻; HRMS-ESI: m/z [M-H]⁻ calcd for C₁₃H₁₃Cl₂FN₇O₄S: 452.0116, found: 452.0115.

N-(3,5-Dibromo-4-fluorophenyl)-4-((2-(1,1-dioxido-1,2,5-thiadiazolidin-2-yl)ethyl)amino)-N'-hydroxy-1,2,5-oxadiazole-3-carboximidamide (7f). ¹H NMR (400 MHz, CD₃CN) δ 9.19 (s, 1H), 7.53 (s, 1H), 7.22 (d, J = 5.5 Hz, 2H), 6.07 (s, 1H), 5.19 (s, 1H), 3.54 (q, J = 6.0 Hz, 2H), 3.49 – 3.37 (m, 4H), 3.26 (t, J = 6.1 Hz, 2H).

^{13}C NMR (126 MHz, CD_3CN) δ 155.34, 151.62 (d, $J = 240.7$ Hz), 140.21, 138.79, 137.31 (d, $J = 3.8$ Hz), 125.91 (2C), 107.78 (d, $J = 23.9$ Hz), 51.29, 49.09, 44.75, 41.94, 39.39. ESI-MS: m/z 540.3 $[\text{M-H}]^-$; HRMS-ESI: m/z $[\text{M-H}]^-$ calcd for $\text{C}_{13}\text{H}_{13}\text{Br}_2\text{FN}_7\text{O}_4\text{S}$: 539.9106, found: 539.9107.

N-(4-Bromo-3-fluorophenyl)-4-((3-(1,1-dioxido-1,2,5-thiadiazolidin-2-yl)propyl)amino)-N'-hydroxy-1,2,5-oxadiazole-3-carboximidamide (8a). To a mixture of **25** (100 mg, 0.45 mmol, 1.0 equiv) and *tert*-butyl (3-bromopropyl)carbamate (161 mg, 0.675 mmol, 1.5 equiv) in dry DMF (2 mL), was added Cs_2CO_3 (440 mg, 1.35 mmol, 3.0 equiv). The reaction was stirred at room temperature overnight, and then the mixture was poured into water and extracted with ethyl acetate. The combined organic phase was washed with water and brine, dried over anhydrous Na_2SO_4 , filtered and concentrated. The resulting residue was purified via silica gel chromatography to give **26a** (123 mg, 72%) as colorless oil. ^1H NMR (300 MHz, CDCl_3) δ 4.75 (s, 1H), 3.79 (td, $J = 6.4, 1.2$ Hz, 2H), 3.32 (t, $J = 6.4$ Hz, 2H), 3.22 (q, $J = 6.4$ Hz, 2H), 3.10 (td, $J = 6.7, 1.2$ Hz, 2H), 1.82 (d, $J = 6.7$ Hz, 2H), 1.53 (s, 9H), 1.42 (s, 9H).

Compound **8a** was obtained from **26a** and **14** by following a similar procedure as that for **5a**. Colorless foam (33%). ^1H NMR (400 MHz, CD_3CN) δ 9.00 (s, 1H), 7.45 (s, 1H), 7.19 (dd, $J = 6.1, 2.6$ Hz, 1H), 7.07 (t, $J = 8.7$ Hz, 1H), 6.99 – 6.83 (m, 1H), 5.93 (t, $J = 5.6$ Hz, 1H), 5.17 (s, 1H), 3.49 – 3.25 (m, 6H), 3.01 (t, $J = 6.9$ Hz, 2H), 1.91 – 1.84 (m, 2H). ^{13}C NMR (126 MHz, CD_3CN) δ 156.86, 156.58 (d, $J = 241.9$ Hz), 142.31, 140.19, 138.15 (d, $J = 2.5$ Hz), 128.52, 124.79 (d, $J = 7.6$ Hz), 116.89 (d, $J = 23.9$ Hz), 108.43 (d, $J = 22.7$ Hz), 50.13, 45.35, 42.63, 40.53, 27.66. ESI-MS: m/z

476.3 [M-H]⁻; HRMS-ESI: *m/z* [M-H]⁻ calcd for C₁₄H₁₆BrFN₇O₄S: 476.0157, found: 476.0154.

N-(4-Bromo-3-fluorophenyl)-4-(((1-((1,1-dioxido-1,2,5-thiadiazolidin-2-yl)methyl)cyclopropyl)methyl)amino)-N'-hydroxy-1,2,5-oxadiazole-3-carboximidamide (8b). To a mixture of **23b** (100 mg, 0.5 mmol, 1.0 equiv) and methanesulfonyl chloride (60 mg, 0.525 mmol, 1.05 equiv) in dry DCM (2 mL), was added Et₃N (61 mg, 0.6 mmol, 1.2 equiv). The reaction was stirred at room temperature for 3 h, and then ethyl acetate and water were added. The organic phase was washed with water and brine, dried over anhydrous Na₂SO₄, filtered and concentrated. The resulting residue **24b** was employed for use without further purification.

Compound **26b** was obtained according to the similar procedure of preparing **26a** using **25** and **24b**. ¹H NMR (300 MHz, CDCl₃) δ 4.91 (s, 1H), 3.81 (t, *J* = 6.4 Hz, 2H), 3.42 (t, *J* = 6.2 Hz, 2H), 3.14 (d, *J* = 6.5 Hz, 2H), 2.98 (s, 2H), 1.55 (s, 9H), 1.43 (s, 9H), 0.66 (t, *J* = 4.9 Hz, 2H), 0.47 (t, *J* = 5.3 Hz, 2H).

Compound **8b** was obtained from **26b** according to a similar procedure as that for **8a**. Faint yellow solid (25%). ¹H NMR (400 MHz, CD₃CN) δ 9.09 (s, 1H), 7.52 (s, 1H), 7.26 (dd, *J* = 6.0, 2.7 Hz, 1H), 7.13 (t, *J* = 8.7 Hz, 1H), 7.02 – 6.93 (m, 1H), 6.14 – 6.04 (m, 1H), 5.19 (s, 1H), 3.52 – 3.37 (m, 4H), 3.34 (d, *J* = 5.9 Hz, 2H), 2.99 (s, 2H), 0.67 (t, *J* = 5.4 Hz, 2H), 0.56 (t, *J* = 5.2 Hz, 2H). ¹³C NMR (126 MHz, CD₃CN) δ 157.23, 156.62 (d, *J* = 241.9 Hz), 142.39, 140.13, 138.15 (d, *J* = 2.5 Hz), 128.57, 124.85 (d, *J* = 7.6 Hz), 116.91 (d, *J* = 23.9 Hz), 108.45 (d, *J* = 21.4 Hz), 52.55, 50.79, 49.78, 40.72, 19.72, 10.09(2C). ESI-MS: *m/z* 502.4 [M-H]⁺; HRMS-ESI: *m/z* [M-H]⁺

calcd for C₁₆H₁₈BrFN₇O₄S: 502.0314, found: 502.0304.

(R)-N-(3-Bromo-4-fluorophenyl)-4-((1-cyclopropyl-2-(1,1-dioxido-1,2,5-thiadiazolidin-2-yl)ethyl)amino)-N'-hydroxy-1,2,5-oxadiazole-3-carboximidamide (8c).

This compound was synthesized as white solid in 21% yield according to a similar protocol as that described for **8a**. ¹H NMR (400 MHz, CD₃CN) δ 9.08 (s, 1H), 7.52 (s, 1H), 7.26 (dd, *J* = 6.0, 2.7 Hz, 1H), 7.12 (t, *J* = 8.7 Hz, 1H), 6.97 (m, 1H), 6.03 (d, *J* = 7.1 Hz, 1H), 5.12 (t, *J* = 8.4 Hz, 1H), 3.57 – 3.49 (m, *J* = 11.2, 7.8 Hz, 1H), 3.46 – 3.31 (m, 5H), 3.20 – 3.10 (m, 1H), 1.19 – 1.07 (m, 1H), 0.64 – 0.52 (m, 2H), 0.48 – 0.34 (m, 2H). ¹³C NMR (126 MHz, CD₃CN) δ 155.65 (d, *J* = 241.9 Hz), 155.52, 141.31, 139.21, 137.18 (d, *J* = 2.9 Hz), 127.57, 123.86 (d, *J* = 7.3 Hz), 115.95 (d, *J* = 23.9 Hz), 107.51 (d, *J* = 22.7 Hz), 58.14, 51.04, 49.91, 40.03, 13.64, 2.59 (2C). ESI-MS: *m/z* 503.8[M+H]⁺; HRMS-ESI: *m/z* [M+H]⁺ calcd for C₁₆H₂₀BrFN₇O₄S: 504.0459, found: 504.0471.

N-(3-Bromo-4-fluorophenyl)-N'-hydroxy-4-((2-(5-(2-methoxyethyl)-1,1-dioxido-1,2,5-thiadiazolidin-2-yl)ethyl)amino)-1,2,5-oxadiazole-3-carboximidamide (9a). To a mixture of sulfamide (1.92 g, 20 mmol, 1.0 equiv) in pyridine (10 mL) at reflux, N¹-benzylethane-1,2-diamine (**27**) (3.0 g, 20 mmol, 1.0 equiv) was added dropwise. The mixture was stirred at reflux for 16 h, and then cooled to room temperature and concentrated. The mixture was poured into water and extracted with ethyl acetate. The organic phase was washed with water and brine, dried over anhydrous Na₂SO₄, filtered and concentrated. The resulting residue was purified via silica gel chromatography to give **28** (3.05 g, 72%) as a slightly brown solid. ¹H NMR

(400 MHz, CDCl₃) δ 7.45 – 7.32 (m, 5H), 4.42 (t, J = 6.6 Hz, 1H), 4.20 (s, 2H), 3.50 (q, J = 6.6 Hz, 2H), 3.30 (t, J = 6.7 Hz, 2H).

To the mixture of **28** (1.0 g, 4.71 mmol, 1.0 equiv) and tert-butyl (2-bromoethyl)carbamate (1.58 g, 7.07 mmol, 1.5 equiv) in dry DMF (5 mL), Cs₂CO₃ (4.6 g, 14.13 mmol, 3.0 equiv) was added. The mixture was stirred at room temperature overnight, and then poured into water and extracted with ethyl acetate. The combined organic phase was washed with water and brine, dried over anhydrous Na₂SO₄, filtered and concentrated. The resulting residue was purified via chromatography to give **29** (1.26 g, 75%) as colorless oil. ¹H NMR (300 MHz, CDCl₃) δ 7.47 – 7.28 (m, 5H), 4.92 (br, 1H), 4.19 (s, 2H), 3.47 – 3.29 (m, 4H), 3.25 – 3.13 (m, 4H), 1.43 (s, 9H).

The mixture of **29** (1.26 g, 3.53 mmol, 1.0 equiv) and 10% Pd(OH)₂ on carbon (600 mg) in MeOH (30 mL) was stirred at 50 °C under a hydrogen atmosphere for 24 h. After filtration, the reaction solution was concentrated and purified via silica gel chromatography to give **30** (815 mg, 87%) as colorless oil. ¹H NMR (300 MHz, CDCl₃) δ 4.94 (s, 1H), 4.53 (s, 1H), 3.60 – 3.28 (m, 6H), 3.16 (t, J = 5.9 Hz, 2H), 1.44 (s, 9H).

To a mixture of **30** (100 mg, 0.377 mmol, 1.0 equiv) and 1-bromo-2-methoxyethane (79 mg, 0.565 mmol, 1.5 equiv) in dry DMF (2 mL), Cs₂CO₃ (370 mg, 1.13 mmol, 3.0 equiv) was added. The reaction was stirred at room temperature overnight and then poured into water. After extraction with ethyl acetate, the organic phase was washed with water and brine, dried over anhydrous Na₂SO₄,

filtered and concentrated. The resulting residue was purified via chromatography to give **32a** (83 mg, 68%) as colorless oil. ^1H NMR (300 MHz, CDCl_3) δ 4.91 (s, 1H), 3.61 (t, $J = 5.1$ Hz, 2H), 3.50 – 3.41 (m, 2H), 3.41 – 3.29 (m, 7H), 3.24 (t, $J = 5.2$ Hz, 2H), 3.17 (t, $J = 6.0$ Hz, 2H), 1.44 (s, 9H).

Compound **9a** was obtained from **14** and **32a** according to a similar procedure as that for preparation of **5a**. White solid (36%). ^1H NMR (400 MHz, CD_3CN) δ 9.14 (s, 1H), 7.51 (s, 1H), 7.25 (dd, $J = 6.0, 2.7$ Hz, 1H), 7.12 (t, $J = 8.7$ Hz, 1H), 7.02 – 6.91 (m, 1H), 6.07 (t, $J = 6.2$ Hz, 1H), 3.55 (m, 4H), 3.40 (s, 4H), 3.34 (s, 3H), 3.28 (t, $J = 6.0$ Hz, 2H), 3.19 – 3.15 (m, 2H). ^{13}C NMR (126 MHz, CD_3CN) δ 156.82, 156.59 (d, $J = 241.9$ Hz), 142.29, 140.23, 138.19 (d, $J = 3.8$ Hz), 128.53, 124.82 (d, $J = 6.3$ Hz), 116.89 (d, $J = 22.7$ Hz), 108.45 (d, $J = 22.7$ Hz), 71.05, 58.86, 48.10, 47.25, 46.88, 46.81, 43.09. ESI-MS: 520.4 $[\text{M}-\text{H}]^-$; HRMS-ESI: m/z $[\text{M}-\text{H}]^-$ calcd for $\text{C}_{16}\text{H}_{20}\text{BrFN}_7\text{O}_5\text{S}$: 520.0420, found: 520.0417.

Compounds **9b-k** were prepared by following procedures similar to that for **9a**.

N-(3-Bromo-4-fluorophenyl)-N'-hydroxy-4-((2-(5-(3-methoxypropyl)-1,1-dioxido-1,2,5-thiadiazolidin-2-yl)ethyl)amino)-1,2,5-oxadiazole-3-carboximidamide (9b). White solid (40%). ^1H NMR (400 MHz, CD_3CN) δ 9.14 (s, 1H), 7.52 (s, 1H), 7.25 (dd, $J = 6.1, 2.7$ Hz, 1H), 7.12 (t, $J = 8.7$ Hz, 1H), 6.96 (m, 1H), 6.06 (t, $J = 5.9$ Hz, 1H), 3.53 (dd, $J = 12.1, 6.1$ Hz, 2H), 3.47 – 3.36 (m, 4H), 3.34 – 3.25 (m, 7H), 3.09 – 3.02 (m, 2H), 1.90 – 1.80 (m, 2H). ^{13}C NMR (126 MHz, CD_3CN) δ 156.81, 156.58 (d, $J = 241.9$ Hz), 142.29, 140.22, 138.19 (d, $J = 3.8$ Hz), 128.50, 124.79 (d, $J = 7.6$ Hz), 116.88 (d, $J = 22.7$ Hz), 108.45 (d, $J = 21.4$ Hz), 70.20, 58.70, 46.94, 46.76,

46.61, 45.79, 43.10, 28.58. ESI-MS: m/z 534.4 [M-H]⁻; HRMS-ESI: m/z [M-H]⁻ calcd for C₁₇H₂₂BrFN₇O₅S: 534.0576, found: 534.0577.

N-(3-Bromo-4-fluorophenyl)-N'-hydroxy-4-((2-(5-(2-hydroxyethyl)-1,1-dioxido-1,2,5-thiadiazolidin-2-yl)ethyl)amino)-1,2,5-oxadiazole-3-carboximidamide (9c). Colorless foam (16%). ¹H NMR (400 MHz, CD₃CN) δ 9.25 (s, 1H), 7.52 (s, 1H), 7.25 (dd, $J = 6.0, 2.7$ Hz, 1H), 7.12 (t, $J = 8.7$ Hz, 1H), 7.02 – 6.90 (m, 1H), 6.09 (t, $J = 6.1$ Hz, 1H), 3.70 (q, $J = 5.6$ Hz, 2H), 3.54 (q, $J = 6.0$ Hz, 2H), 3.41 (s, 4H), 3.29 (t, $J = 6.0$ Hz, 2H), 3.11 (t, $J = 5.5$ Hz, 2H), 3.05 (t, $J = 5.8$ Hz, 1H). ¹³C NMR (126 MHz, CD₃CN) δ 156.80, 156.55 (d, $J = 241.9$ Hz), 142.23, 140.22, 138.19 (d, $J = 2.5$ Hz), 128.47, 124.76 (d, $J = 7.6$ Hz), 116.87 (d, $J = 23.9$ Hz), 108.43 (d, $J = 21.4$ Hz), 60.43, 50.67, 47.00, 46.85, 46.74, 42.99. ESI-MS: m/z 506.4 [M-H]⁻; HRMS-ESI: m/z [M-H]⁻ calcd for C₁₅H₁₈BrFN₇O₅S: 506.0263, found: 506.0259.

N-(3-Bromo-4-fluorophenyl)-N'-hydroxy-4-((2-(5-(2-(2-(2-hydroxyethoxy)ethoxy)ethyl)-1,1-dioxido-1,2,5-thiadiazolidin-2-yl)ethyl)amino)-1,2,5-oxadiazole-3-carboximidamide (9d). Colorless foam (25%). ¹H NMR (400 MHz, CD₃CN) δ 9.30 (s, 1H), 7.52 (s, 1H), 7.24 (dd, $J = 4.0, 1.6$ Hz, 1H), 7.12 (t, $J = 8.6$ Hz, 1H), 7.02 – 6.86 (m, 1H), 6.09 (t, $J = 5.1$ Hz, 1H), 3.68 (t, $J = 4.9$ Hz, 2H), 3.65-3.57 (m, 6H), 3.54 (dd, $J = 9.1, 4.3$ Hz, 4H), 3.48 – 3.34 (m, 4H), 3.28 (t, $J = 5.6$ Hz, 2H), 3.18 (t, $J = 4.7$ Hz, 2H), 2.90 (s, 1H). ¹³C NMR (126 MHz, CD₃CN) δ 156.78, 156.55 (d, $J = 241.9$ Hz), 142.24, 140.23, 138.19 (d, $J = 2.5$ Hz), 128.45, 124.75 (d, $J = 7.6$ Hz), 116.87 (d, $J = 22.7$ Hz), 108.44 (d, $J = 21.4$ Hz), 73.21, 71.05, 70.93, 69.66, 62.00, 48.17, 47.26, 46.82, 46.81, 43.06. ESI-MS: m/z 594.5 [M-H]⁻; HRMS-ESI: m/z

[M-H]⁻ calcd for C₁₉H₂₆BrFN₇O₇S: 594.0787, found: 594.0778.

N-(3-Bromo-4-fluorophenyl)-N'-hydroxy-4-((2-(5-((3-(hydroxymethyl)oxetan-3-yl)methyl)-1,1-dioxido-1,2,5-thiadiazolidin-2-yl)ethyl)amino)-1,2,5-oxadiazole-3-carboximidamide (9e). Faint yellow foam (20%). ¹H NMR (400 MHz, CD₃CN) δ 9.19 (dd, *J* = 6.1, 4.4 Hz, 1H), 7.52 (s, 1H), 7.25 (dd, *J* = 6.1, 2.7 Hz, 1H), 7.12 (t, *J* = 8.7 Hz, 1H), 7.01 – 6.92 (m, 1H), 6.08 (t, *J* = 6.3 Hz, 1H), 4.45 (d, *J* = 6.3 Hz, 2H), 4.38 (d, *J* = 6.3 Hz, 2H), 3.80 (d, *J* = 5.4 Hz, 2H), 3.55 (dd, *J* = 12.1, 6.0 Hz, 2H), 3.40 (dd, *J* = 7.8, 5.2 Hz, 6H), 3.29 (t, *J* = 6.0 Hz, 2H), 3.16 – 3.08 (m, 1H). ¹³C NMR (126 MHz, CD₃CN) δ 156.81, 156.58 (d, *J* = 241.9 Hz), 142.30, 140.23, 138.19 (d, *J* = 2.5 Hz), 128.52, 124.80 (d, *J* = 7.6 Hz), 116.89 (d, *J* = 22.7 Hz), 108.45 (d, *J* = 22.7 Hz), 76.94 (2C), 64.51, 51.16, 48.68, 46.82, 46.60, 45.20, 42.98. ESI-MS: *m/z* 562.4 [M-H]⁻; HRMS-ESI: *m/z* [M-H]⁻ calcd for C₁₈H₂₂BrFN₇O₆S: 562.0525, found: 562.0521.

N-(3-Bromo-4-fluorophenyl)-4-((2-(5-(2-(dimethylamino)ethyl)-1,1-dioxido-1,2,5-thiadiazolidin-2-yl)ethyl)amino)-N'-hydroxy-1,2,5-oxadiazole-3-carboximidamide (9f). White solid (30%). ¹H NMR (400 MHz, CD₃CN) δ 7.50 (s, 1H), 7.21 (dd, *J* = 6.0, 2.6 Hz, 1H), 7.10 (t, *J* = 8.7 Hz, 1H), 7.00 – 6.85 (m, 1H), 6.15 (t, *J* = 6.1 Hz, 1H), 3.52 (dd, *J* = 11.4, 5.8 Hz, 2H), 3.47 – 3.37 (m, 4H), 3.36 – 3.28 (m, 2H), 3.20 (t, *J* = 6.8 Hz, 2H), 2.74 (t, *J* = 6.9 Hz, 2H), 2.33 (s, 6H). ¹³C NMR (126 MHz, CD₃CN) δ 156.82, 156.37 (d, *J* = 240.7 Hz), 141.96, 140.43, 138.43 (d, *J* = 3.8 Hz), 128.09, 124.36 (d, *J* = 7.6 Hz), 116.84 (d, *J* = 23.9 Hz), 108.41 (d, *J* = 22.7 Hz), 56.76, 46.91, 46.67, 45.75, 45.64, 45.03 (2C), 42.38. ESI-MS: 533.4 [M-H]⁻; HRMS-ESI: *m/z*

[M-H]⁻ calcd for C₁₇H₂₃BrFN₈O₄S: 533.0736, found: 533.0742.

N-(3-Bromo-4-fluorophenyl)-N'-hydroxy-4-((2-(5-(2-morpholinoethyl)-1,1-dioxido-1,2,5-thiadiazolidin-2-yl)ethyl)amino)-1,2,5-oxadiazole-3-carboximidamide (9g). White solid (38%). ¹H NMR (400 MHz, CD₃CN) δ 7.53 (s, 1H), 7.21 (dd, *J* = 6.0, 2.7 Hz, 1H), 7.09 (t, *J* = 8.7 Hz, 1H), 6.92 (ddd, *J* = 8.8, 4.1, 2.8 Hz, 1H), 6.05 (t, *J* = 6.0 Hz, 1H), 3.69 – 3.58 (m, 4H), 3.50 (dd, *J* = 11.8, 5.9 Hz, 2H), 3.45 – 3.34 (m, 4H), 3.28 (t, *J* = 5.9 Hz, 2H), 3.16 (t, *J* = 6.9 Hz, 2H), 2.64 (t, *J* = 6.9 Hz, 2H), 2.43-2.53 (m, 4H). ¹³C NMR (126 MHz, CD₃CN) δ 155.85, 155.54 (d, *J* = 241.9 Hz), 141.23, 139.35, 137.35 (d, *J* = 2.5 Hz), 127.41, 123.69 (d, *J* = 6.3 Hz), 115.92 (d, *J* = 23.9 Hz), 107.48 (d, *J* = 21.4 Hz), 66.09(2C), 55.95, 53.33(2C), 46.08, 45.51, 45.33, 45.23, 41.75. ESI-MS: *m/z* 575.5 [M-H]⁻; HRMS-ESI: *m/z* [M-H]⁻ calcd for C₁₉H₂₅BrFN₈O₅S: 575.0842, found: 575.0838.

4-((2-(5-Benzyl-1,1-dioxido-1,2,5-thiadiazolidin-2-yl)ethyl)amino)-N-(3-bromo-4-fluorophenyl)-N'-hydroxy-1,2,5-oxadiazole-3-carboximidamide (9h). White solid (36%). ¹H NMR (400 MHz, CD₃CN) δ 9.07 (s, 1H), 7.50 (s, 1H), 7.41 – 7.29 (m, 5H), 7.22 (dd, *J* = 6.0, 2.7 Hz, 1H), 7.08 (t, *J* = 8.7 Hz, 1H), 6.98 – 6.88 (m, 1H), 6.06 (t, *J* = 5.8 Hz, 1H), 4.15 (s, 2H), 3.53 (q, *J* = 6.1 Hz, 2H), 3.37 (t, *J* = 6.5 Hz, 2H), 3.28 (t, *J* = 6.0 Hz, 2H), 3.20 (t, *J* = 6.4 Hz, 2H). ¹³C NMR (126 MHz, CD₃CN) δ 155.87, 155.63 (d, *J* = 241.9 Hz), 141.35, 139.28, 137.23 (d, *J* = 3.8 Hz), 135.83, 128.60(4C), 127.88, 127.58, 123.87 (d, *J* = 6.3 Hz), 115.93 (d, *J* = 22.7 Hz), 107.49 (d, *J* = 22.7 Hz), 51.14, 46.07, 45.78, 45.31, 42.19. ESI-MS: *m/z* 552.4 [M-H]⁻; HRMS calcd for C₂₀H₂₀BrFN₇O₄S: 552.0467, found: 552.0464.

(3-Bromo-4-fluorophenyl)-4-((2-(5-((2-bromopyridin-4-yl)methyl)-1,1-dioxido-1,2,5-thiadiazolidin-2-yl)ethyl)amino)-*N'*-hydroxy-1,2,5-oxadiazole-3-carboximidamide (9i). White solid (40%). ¹H NMR (400 MHz, CD₃CN) δ 9.28 – 9.02 (m, 1H), 8.34 (d, *J* = 5.3 Hz, 1H), 7.59 (s, 1H), 7.53 (s, 1H), 7.39 (d, *J* = 5.0 Hz, 1H), 7.24 (dd, *J* = 5.9, 2.3 Hz, 1H), 7.11 (td, *J* = 8.3, 1.6 Hz, 1H), 6.95 (dt, *J* = 5.6, 3.7 Hz, 1H), 6.09 (s, 1H), 4.21 (s, 2H), 3.56 (q, *J* = 5.9 Hz, 2H), 3.45 (t, *J* = 6.4 Hz, 2H), 3.32 (t, *J* = 6.1 Hz, 4H). ¹³C NMR (126 MHz, CD₃CN) δ 155.86, 155.63 (d, *J* = 241.9 Hz), 150.40, 149.06, 141.97, 141.37, 139.27, 137.21 (d, *J* = 3.8 Hz), 127.58, 127.19, 123.86 (d, *J* = 7.6 Hz), 122.57, 115.94 (d, *J* = 23.9 Hz), 107.50 (d, *J* = 22.7 Hz), 49.69, 46.03, 45.97, 45.73, 42.13. ESI-MS: 631.3 [M-H]⁻; HRMS-ESI: *m/z* [M-H]⁻ calcd for C₁₉H₁₈Br₂FN₈O₄S: 630.9528, found: 630.9536.

***N*-(3-Bromo-4-fluorophenyl)-4-((2-(5-((3,3-difluorocyclobutyl)methyl)-1,1-dioxido-1,2,5-thiadiazolidin-2-yl)ethyl)amino)-*N'*-hydroxy-1,2,5-oxadiazole-3-carboximidamide (9j).** White solid (46%). ¹H NMR (400 MHz, CD₃CN) δ 9.03 (s, 1H), 7.50 (s, 1H), 7.23 (dd, *J* = 6.1, 2.7 Hz, 1H), 7.11 (t, *J* = 8.8 Hz, 1H), 6.95 (m, 1H), 6.04 (t, *J* = 6.0 Hz, 1H), 3.53 (dd, *J* = 12.2, 6.1 Hz, 2H), 3.45 – 3.23 (m, 6H), 3.10 (d, *J* = 7.4 Hz, 2H), 2.78 – 2.62 (m, 2H), 2.51 – 2.25 (m, 3H). ¹³C NMR (126 MHz, CD₃CN) δ 155.85, 155.56 (d, *J* = 241.9 Hz), 141.22, 139.30, 137.31, 127.42, 123.72 (d, *J* = 7.6 Hz), 115.93 (d, *J* = 23.9 Hz), 107.48 (d, *J* = 22.7 Hz), 51.74, 46.04(2C), 45.82, 42.08, 38.50 (t, *J* = 22.7 Hz, 2C), 21.55 (q, *J* = 6.3 Hz). ESI-MS: 566.4 [M-H]⁻; HRMS-ESI: *m/z* [M-H]⁻ calcd for C₁₈H₂₀BrF₃N₇O₄S: 566.0438, found: 566.0433.

***N*-(3-Bromo-4-fluorophenyl)-4-((2-(5-(2,2-difluoroethyl)-1,1-dioxido-1,2,5-thi**

adiazolidin-2-yl)ethyl)amino)-N'-hydroxy-1,2,5-oxadiazole-3-carboximidamide

(9k). Faint yellow foam (20%). ¹H NMR (400 MHz, CD₃CN) δ 9.05 (s, 1H), 7.51 (s, 1H), 7.25 (dd, *J* = 6.0, 2.8 Hz, 1H), 7.12 (t, *J* = 8.7 Hz, 1H), 6.99 – 6.86 (m, 1H), 6.27 – 5.88 (m, 3H), 3.56 (dd, *J* = 12.3, 6.0 Hz, 2H), 3.50 – 3.42 (m, 4H), 3.29 (t, *J* = 6.1 Hz, 2H). ¹³C NMR (126 MHz, CD₃CN) δ 156.76, 156.56 (d, *J* = 241.9 Hz), 142.26, 140.18, 138.12 (d, *J* = 2.5 Hz), 128.49, 124.78 (d, *J* = 7.6 Hz), 116.86 (d, *J* = 22.7 Hz), 115.54 (t, *J* = 240.7 Hz), 108.43 (d, *J* = 22.7 Hz), 50.41 (t, *J* = 26.5 Hz), 48.48, 46.88, 46.76, 43.02. ESI-MS: 526.4 [M-H]⁻; HRMS-ESI: *m/z* [M-H]⁻ calcd for C₁₅H₁₆BrF₃N₇O₄S: 526.0125, found: 526.0124.

2-(5-(2-((4-(N-(3-bromo-4-fluorophenyl)-N'-hydroxycarbamimidoyl)-1,2,5-oxadiazol-3-yl)amino)ethyl)-1,1-dioxido-1,2,5-thiadiazolidin-2-yl)ethyl

(S)-3-fluoropyrrolidine-1-carboxylate (9l). To a mixture of **30** (100 mg, 0.377 mmol, 1.0 equiv) and 1,2-dibromoethane (85 mg, 0.452 mmol, 1.2 equiv) in dry DMF (2 mL), Cs₂CO₃ (246 mg, 0.754 mmol, 2.0 equiv) was added. The reaction was stirred at room temperature overnight, and then poured into water and extracted with ethyl acetate. The organic phase was washed with water and brine, dried over anhydrous Na₂SO₄, filtered and concentrated. The resulting residue was purified via chromatography to give **31** (63 mg, 45%) as colorless oil. ¹H NMR (300 MHz, CDCl₃) δ 4.87 (s, 1H), 3.57 – 3.28 (m, 10H), 3.17 (t, *J* = 5.9 Hz, 2H), 1.44 (s, 9H).

To the mixture of **31** (50 mg, 0.134 mmol, 1.0 equiv) and (S)-(+)-3-fluoropyrrolidine hydrochloride (25 mg, 0.202 mmol, 1.5 equiv) in dry DMF (2 mL), Cs₂CO₃ (130 mg, 0.4 mmol, 3.0 equiv) was added. The reaction was

stirred at 60 °C for 2 h and then poured into water and extracted with ethyl acetate. The combined organic phase was washed with water and brine, dried over anhydrous Na₂SO₄, filtered and concentrated. The resulting residue was purified via chromatography to give **321** (21 mg, 37%) as colorless oil. ¹H NMR (400 MHz, CDCl₃) δ 5.26 (d, *J* = 52.1 Hz, 1H), 4.92 (s, 1H), 4.41 – 4.23 (m, 2H), 3.85 – 3.31 (m, 11H), 3.18 (t, *J* = 5.9 Hz, 2H), 2.35 – 2.20 (m, 1H), 2.13 – 1.91 (m, 1H), 1.52 – 1.41 (m, 9H).

Compound **9l** was prepared from **14** and **321** by following similar procedures as that for **5a**. White solid (30%). ¹H NMR (400 MHz, CD₃CN) δ 9.29 (dd, *J* = 6.4, 3.6 Hz, 1H), 7.52 (s, 1H), 7.25 (dd, *J* = 6.0, 2.7 Hz, 1H), 7.12 (t, *J* = 8.7 Hz, 1H), 7.01 – 6.92 (m, 1H), 6.08 (t, *J* = 6.1 Hz, 1H), 5.27 (dd, *J* = 52.9, 3.5 Hz, 1H), 4.31 – 4.18 (m, 2H), 3.72 – 3.35 (m, 10H), 3.28 (dt, *J* = 11.9, 5.3 Hz, 4H), 2.17 – 2.01 (m, 2H). ¹³C NMR (126 MHz, CD₃CN) δ 156.81, 156.58 (d, *J* = 241.9 Hz), 155.47 (d, *J* = 16.4 Hz), 142.29, 140.25, 138.21 (d, *J* = 2.5 Hz), 128.51, 124.79 (d, *J* = 7.8 Hz), 116.89 (d, *J* = 22.7 Hz), 108.54 (d, *J* = 22.7 Hz), 94.03 (q, *J* = 69.3 Hz), 63.67, 63.63, 53.61 (d, *J* = 16.4 Hz), 47.94, 47.18, 46.83, 46.76, 44.65 (d, *J* = 40.3 Hz), 32.54 (dd, *J* = 21.4, 94.5 Hz). ESI-MS: *m/z* 621.5 [M-H]⁻; HRMS-ESI: *m/z* [M-H]⁻ calcd for C₂₀H₂₄BrF₂N₈O₆S: 621.0696, found: 621.0699.

2-(5-(2-((4-(N-(3-Bromo-4-fluorophenyl)-N'-hydroxycarbamimidoyl)-1,2,5-oxadiazol-3-yl)amino)ethyl)-1,1-dioxido-1,2,5-thiadiazolidin-2-yl)ethyl

3-methoxyazetidine-1-carboxylate (9m). This compound was synthesized according to a similar protocol as that described for **9l**. White solid (34%). ¹H NMR (400 MHz,

CD₃CN) δ 9.40 (s, 1H), 7.51 (s, 1H), 7.23 (dd, $J = 6.1, 2.7$ Hz, 1H), 7.11 (t, $J = 8.7$ Hz, 1H), 6.95 (m, 1H), 6.09 (t, $J = 5.8$ Hz, 1H), 4.24 – 4.00 (m, 5H), 3.87 – 3.71 (m, 2H), 3.53 (dd, $J = 12.0, 6.0$ Hz, 2H), 3.47 – 3.35 (m, 4H), 3.32 – 3.20 (m, 7H). ¹³C NMR (126 MHz, CD₃CN) δ 157.38, 156.78, 156.53 (d, $J = 241.9$ Hz), 142.23, 140.22, 138.19 (d, $J = 2.5$ Hz), 128.44, 124.73 (d, $J = 7.6$ Hz), 116.86 (d, $J = 23.9$ Hz), 108.42 (d, $J = 22.7$ Hz), 70.10, 63.33 (2C), 56.25, 47.79 (2C), 47.07, 46.74, 46.68, 42.90. ESI-MS: m/z 619.4 [M-H]⁻; HRMS-ESI: m/z [M-H]⁻ calcd for C₂₀H₂₅BrFN₈O₇S: 619.0744, found: 619.0744.

5.2. hIDO1 enzymatic assay

The hIDO1 enzymatic assay was performed as described previously⁴². Briefly, a standard reaction mixture (30 μ L) containing 100 mM potassium phosphate buffer (pH 6.5), 40 mmol/L ascorbic acid and 0.01% Triton X-100, 200 μ g/mL catalase, 20 μ mol/L methylene blue and 0.05 μ M rhIDO-1 was added to the solution (60 μ L) containing the substrate L-tryptophan (250 μ mol/L) and the test sample at a determined concentration. The reaction was carried out at 37 °C for 30 min and stopped by adding 45 μ L of 30% (w/v) trichloroacetic acid. After being heated at 65 °C for 15 min, the reaction mixture was centrifuged at 12000 rpm for 10 min. The supernatant (100 μ L) was transferred into a well of a 96-well microplate and mixed with 100 μ L of 2% (w/v) p-dimethylamino benzaldehyde in acetic acid. The yellow pigment derived from kynurenine was measured at 492 nm using a SpectraMax Plus 384 microplate reader (Molecular_Devices, Sunnyvale, CA). IC₅₀ values were calculated by using GraphPad Prism 6 software (San Diego, California USA).

5.3. Cell-based assay of IDO1 inhibitors

The cellular activity of IDO1 was detected as described previously⁴². HEK 293 cells were seeded in a 6-well culture plate at a density of 5×10^5 cells/well and cultured overnight. After 24 h, HEK 293 cells were transfected with pcDNA3.1-hIDO1 using lipofectamine 2000 according to the manufacturer's instructions. Cells were seeded in a 96-well culture plate at a density of 2.5×10^4 cells/well. After 24 h transfection, a serial dilution of the tested compounds in 10 μ L PBS was added to the cells. After an additional 12-h incubation, 200 μ L of the supernatant per well was transferred to a new 96-well plate and mixed with 100 μ L of 30% trichloroacetic acid in each well, and the plate was incubated at 65 °C for 15 min to hydrolyze *N*-formylkynurenine produced by the catalytic reaction of hIDO1. The reaction mixture was then centrifuged for 10 min at 12000 rpm to remove the sediments. Then 100 μ L of the supernatant per well were transferred to another 96-well plate and mixed with 100 μ L of 2% (w/v) *p*-dimethylamino benzaldehyde in acetic acid. The yellow color derived from kynurenine was measured at 492 nm using a SpectraMax Plus 384 microplate reader (Molecular Devices, Sunnyvale, CA).

5.4. Pharmacokinetic parameters in rats

Tested compounds were administrated to male Sprague-Dawley (SD) rats ($n = 3$) by gavage either as a solution of 1 mg/kg in DMSO/EtOH/PEG300/NaCl (5/5/40/50, v/v/v/v) intravenously or as a suspension of 3 mg/kg in DMSO/0.5% HPMC (5/95, v/v/) orally. Blood samples were collected at 0.05, 0.25, 0.75, 2, 4, 8 and 24 h after intravenous dosing while 0.25, 0.5, 1, 2, 4, 8 and 24 h following oral dosing. The

blood samples were placed on wet ice, and serum was collected after 2 centrifugation. Serum samples were frozen and stored at -20 °C. The serum samples were analyzed utilizing HPLC-coupled tandem mass spectrometry (LC-MS/MS).

All animal experiments were performed according to the institutional ethical guidelines on animal care and approved by the Institute Animal Care and Use Committee at Shanghai Institute of *Materia Medica*.

5.5. *In vivo antitumor activity assay*

Female BALB/c mice (4–6 weeks old) were housed and maintained under specific pathogen-free conditions. Animal procedures were performed according to institutional ethical guidelines of animal care. The CT26 tumor cells (ATCC-CRL-2638) were maintained *in vitro* as a monolayer culture in RPMI-1640 medium supplemented with 10% heat inactivated fetal bovine serum (Gibco product), 100 U/mL penicillin and 100 µg/mL streptomycin at 37 °C in an atmosphere of 5 % CO₂ in air. The tumor cells were routinely subcultured twice weekly by trypsin-EDTA treatment. The cells growing in an exponential growth phase were harvested and counted for tumor inoculation. Each mouse was inoculated subcutaneously at the right lower flank with CT26 tumor cells (0.3×10^6 /mouse) in 0.1 mL of PBS for tumor development. Treatments were started on day 8 after tumor inoculation when the average tumor size reached approximately 49 mm³. The animals were assigned into groups using an Excel-based randomization software performing stratified randomization based upon their tumor volumes. Each group consisted of 8 tumor-bearing mice. The control groups were given vehicle alone, and the treatment

groups were given compounds showed in Figure 3 and Figure 4. Tumor size was measured thrice weekly in two dimensions using a caliper, and the volume was expressed in mm^3 using the formula: $V = 0.5 a * b^2$ where a and b are the long and short diameters of the tumor, respectively. The tumor size was then used for calculations of T/C values. The T/C value (in percent) is an indication of antitumor effectiveness; T and C are the mean volumes of the treated and control groups, respectively, on a given day. TGI was calculated for each group using the formula: $\text{TGI (\%)} = [1 - (T_i - T_0) / (V_i - V_0)] \times 100$; T_i is the average tumor volume of a treatment group on a given day, T_0 is the average tumor volume of the treatment group on day 0, V_i is the average tumor volume of the vehicle control group on the same day with T_i , and V_0 is the average tumor volume of the vehicle group on day 0.

All the procedures related to animal handling, care and the treatment in the study were performed according to the guidelines approved by the Institutional Animal Care and Use Committee (IACUC) of WuXi AppTec following the guidance of the Association for Assessment and Accreditation of Laboratory Animal Care (AAALAC).

5.6. Statistical analysis

Summary statistics, including mean and the standard error of the mean (SEM), are provided for the tumor volume of each group at each time point. Statistical analysis of difference in the tumor volume among the groups were conducted on the data obtained at the best therapeutic time point (the 14th day after grouping). A one-way ANOVA was performed to compare the tumor volume among groups, and when a significant F-statistics (a ratio of treatment variance to the error variance) was obtained, comparisons between groups were carried out with Games-Howell test. The

event of interest is the animal death. The survival time is defined as the time from the start of dosing to the tumor volume reaches 3000mm^3 . For each group, the median survival time and corresponding 95% confidence interval were calculated. The Kaplan-Meier curves were also constructed for each group and the log-rank test was used to compare survival curves between groups. All data were analyzed using SPSS 17.0. $p < 0.05$ was considered to be statistically significant.

6. Acknowledgement

This work was supported by grants from Chinese NSF (Grants 81430080, 81773565, 81703327). Supporting grants from the Key Program of the Frontier Science (Grant 160621) of the Chinese Academy of Sciences, the Shanghai Commission of Science and Technology (Grants 16XD1404600, 14431900400) are also appreciated. We thank Professor Zhaobing Gao and Dr. Xueqin Chen for conducting the hERG test.

7. Abbreviations used

IDO1, indoleamine 2, 3-dioxygenase 1; PD-1, programmed death receptor 1; PD-L1, programmed death receptor ligand 1; CTLA-4, cytotoxic T lymphocyte associated protein 4; Kyn, kynurenine; TRP, tryptophan; NFK, *N*-formyl kynurenine; GCN2, general control non-derepressible 2; AhR, aryl hydrocarbon receptor; mTOR, mechanistic target of rapamycin; PK, pharmacokinetic; V_{ss} , volume of distribution; $T_{1/2}$, half-life; C_{max} , maximum concentration; T_{max} , time of maximum concentration; $AUC_{0-\infty}$, area under the plasma concentration time curve; F , oral bioavailability; TGI, tumor growth inhibition; T/C, treatment/control; MST, median survival time; ILS, increase in life-span; TFA, trifluoroacetic acid; CDI, 1,1'-carbonyldiimidazole; AAALAC, the association for assessment and accreditation of laboratory animal care; IACUC, the institutional animal care and use committee.

8. References

1. Emens, L. A.; Ascierto, P. A.; Darcy, P. K.; Demaria, S.; Eggermont, A. M. M.; Redmond, W. L.; Seliger, B.; Marincola, F. M., Cancer immunotherapy: Opportunities and challenges in the rapidly evolving clinical landscape. *Eur J Cancer* **2017**, *81*, 116-129.
2. Sharma, P.; Allison, J. P., The future of immune checkpoint therapy. *Science* **2015**, *348* (6230), 56-61.
3. Reck, M.; Rodriguez-Abreu, D.; Robinson, A. G.; Hui, R.; Czoszi, T.; Fulop, A.; Gottfried, M.; Peled, N.; Tafreshi, A.; Cuffe, S.; O'Brien, M.; Rao, S.; Hotta, K.; Leiby, M. A.; Lubiniecki, G. M.; Shentu, Y.; Rangwala, R.; Brahmer, J. R.; Investigators, K.-. Pembrolizumab versus Chemotherapy for PD-L1-Positive Non-Small-Cell Lung Cancer. *N Engl J Med* **2016**, *375* (19), 1823-1833.
4. Eggermont, A. M.; Chiarion-Sileni, V.; Grob, J. J.; Dummer, R.; Wolchok, J. D.; Schmidt, H.; Hamid, O.; Robert, C.; Ascierto, P. A.; Richards, J. M.; Lebbe, C.; Ferraresi, V.; Smylie, M.; Weber, J. S.; Maio, M.; Bastholt, L.; Mortier, L.; Thomas, L.; Tahir, S.; Hauschild, A.; Hassel, J. C.; Hodi, F. S.; Taitt, C.; de Pril, V.; de Schaetzen, G.; Suci, S.; Testori, A., Prolonged Survival in Stage III Melanoma with Ipilimumab Adjuvant Therapy. *N Engl J Med* **2016**, *375* (19), 1845-1855.
5. Weber, J.; Mandala, M.; Del Vecchio, M.; Gogas, H. J.; Arance, A. M.; Cowey, C. L.; Dalle, S.; Schenker, M.; Chiarion-Sileni, V.; Marquez-Rodas, I.; Grob, J. J.; Butler, M. O.; Middleton, M. R.; Maio, M.; Atkinson, V.; Queirolo, P.; Gonzalez, R.; Kudchadkar, R. R.; Smylie, M.; Meyer, N.; Mortier, L.; Atkins, M. B.; Long, G. V.; Bhatia, S.; Lebbe, C.; Rutkowski, P.; Yokota, K.; Yamazaki, N.; Kim, T. M.; de Pril, V.; Sabater, J.; Qureshi, A.; Larkin, J.; Ascierto, P. A.; CheckMate, C., Adjuvant Nivolumab versus Ipilimumab in Resected Stage III or IV Melanoma. *N Engl J Med* **2017**, *377* (19), 1824-1835.
6. Yue, E. W.; Sparks, R.; Polam, P.; Modi, D.; Douty, B.; Wayland, B.; Glass, B.;

- Takvorian, A.; Glenn, J.; Zhu, W.; Bower, M.; Liu, X.; Leffet, L.; Wang, Q.; Bowman, K. J.; Hansbury, M. J.; Wei, M.; Li, Y.; Wynn, R.; Burn, T. C.; Koblisch, H. K.; Fridman, J. S.; Emm, T.; Scherle, P. A.; Metcalf, B.; Combs, A. P., INCB24360 (Epcadostat), a Highly Potent and Selective Indoleamine-2,3-dioxygenase 1 (IDO1) Inhibitor for Immuno-oncology. *ACS Med Chem Lett* **2017**, 8 (5), 486-491.
7. Garon, E. B.; Rizvi, N. A.; Hui, R.; Leighl, N.; Balmanoukian, A. S.; Eder, J. P.; Patnaik, A.; Aggarwal, C.; Gubens, M.; Horn, L.; Carcereny, E.; Ahn, M. J.; Felip, E.; Lee, J. S.; Hellmann, M. D.; Hamid, O.; Goldman, J. W.; Soria, J. C.; Dolled-Filhart, M.; Rutledge, R. Z.; Zhang, J.; Luceford, J. K.; Rangwala, R.; Lubiniecki, G. M.; Roach, C.; Emancipator, K.; Gandhi, L.; Investigators, K.-. Pembrolizumab for the treatment of non-small-cell lung cancer. *N Engl J Med* **2015**, 372 (21), 2018-28.
8. Carvalho, S.; Levi-Schaffer, F.; Sela, M.; Yarden, Y., Immunotherapy of cancer: from monoclonal to oligoclonal cocktails of anti-cancer antibodies: IUPHAR Review 18. *Br J Pharmacol* **2016**, 173 (9), 1407-24.
9. Munn, D. H.; Mellor, A. L., IDO and tolerance to tumors. *Trends Mol Med* **2004**, 10 (1), 15-8.
10. Rohrig, U. F.; Majjigapu, S. R.; Vogel, P.; Zoete, V.; Michielin, O., Challenges in the Discovery of Indoleamine 2,3-Dioxygenase 1 (IDO1) Inhibitors. *J Med Chem* **2015**, 58 (24), 9421-37.
11. Dounay, A. B.; Tuttle, J. B.; Verhoest, P. R., Challenges and Opportunities in the Discovery of New Therapeutics Targeting the Kynurenine Pathway. *J Med Chem* **2015**, 58 (22), 8762-82.
12. Macchiarulo, A.; Camaioni, E.; Nuti, R.; Pellicciari, R., Highlights at the gate of tryptophan catabolism: a review on the mechanisms of activation and regulation of indoleamine 2,3-dioxygenase (IDO), a novel target in cancer disease. *Amino Acids* **2009**, 37 (2), 219-29.

13. Munn, D. H.; Mellor, A. L., Indoleamine 2,3 dioxygenase and metabolic control of immune responses. *Trends Immunol* **2013**, *34* (3), 137-43.
14. van Baren, N.; Van den Eynde, B. J., Tryptophan-degrading enzymes in tumoral immune resistance. *Front Immunol* **2015**, *6*, 34.
15. Munn, D. H.; Mellor, A. L., IDO in the Tumor Microenvironment: Inflammation, Counter-Regulation, and Tolerance. *Trends Immunol* **2016**, *37* (3), 193-207.
16. Godin-Ethier, J.; Hanafi, L. A.; Piccirillo, C. A.; Lapointe, R., Indoleamine 2,3-dioxygenase expression in human cancers: clinical and immunologic perspectives. *Clin Cancer Res* **2011**, *17* (22), 6985-91.
17. Lin, S. Y.; Yeh, T. K.; Kuo, C. C.; Song, J. S.; Cheng, M. F.; Liao, F. Y.; Chao, M. W.; Huang, H. L.; Chen, Y. L.; Yang, C. Y.; Wu, M. H.; Hsieh, C. L.; Hsiao, W.; Peng, Y. H.; Wu, J. S.; Lin, L. M.; Sun, M.; Chao, Y. S.; Shih, C.; Wu, S. Y.; Pan, S. L.; Hung, M. S.; Ueng, S. H., Phenyl Benzenesulfonylhydrazides Exhibit Selective Indoleamine 2,3-Dioxygenase Inhibition with Potent in Vivo Pharmacodynamic Activity and Antitumor Efficacy. *J Med Chem* **2016**, *59* (1), 419-30.
18. Malachowski, W. P.; Winters, M.; DuHadaway, J. B.; Lewis-Ballester, A.; Badir, S.; Wai, J.; Rahman, M.; Sheikh, E.; LaLonde, J. M.; Yeh, S. R.; Prendergast, G. C.; Muller, A. J., O-alkylhydroxylamines as rationally-designed mechanism-based inhibitors of indoleamine 2,3-dioxygenase-1. *Eur J Med Chem* **2016**, *108*, 564-576.
19. Paul, S.; Roy, A.; Deka, S. J.; Panda, S.; Trivedi, V.; Manna, D., Nitrobenzofurazan derivatives of N'-hydroxyamidines as potent inhibitors of indoleamine-2,3-dioxygenase 1. *Eur J Med Chem* **2016**, *121*, 364-375.
20. Crosignani, S.; Bingham, P.; Bottemanne, P.; Cannelle, H.; Cauwenberghs, S.; Cordonnier, M.; Dalvie, D.; Deroose, F.; Feng, J. L.; Gomes, B.; Greasley, S.; Kaiser, S. E.; Kraus, M.; Negrierie, M.; Maegley, K.; Miller, N.; Murray, B. W.; Schneider, M.; Soloweij, J.; Stewart, A. E.; Tumang, J.; Torti, V. R.; Van Den Eynde, B.; Wythes, M., Discovery of a Novel and Selective Indoleamine

- 2,3-Dioxygenase (IDO-1) Inhibitor
3-(5-Fluoro-1H-indol-3-yl)pyrrolidine-2,5-dione (EOS200271/PF-06840003) and
Its Characterization as a Potential Clinical Candidate. *J Med Chem* **2017**, *60* (23),
9617-9629.
21. Brant, M. G.; Goodwin-Tindall, J.; Stover, K. R.; Stafford, P. M.; Wu, F.; Meek,
A. R.; Schiavini, P.; Wohnig, S.; Weaver, D. F., Identification of Potent
Indoleamine 2,3-Dioxygenase 1 (IDO1) Inhibitors Based on a Phenylimidazole
Scaffold. *ACS Med Chem Lett* **2018**, *9* (2), 131-136.
22. Fang, K.; Dong, G.; Li, Y.; He, S.; Wu, Y.; Wu, S.; Wang, W.; Sheng, C.,
Discovery of Novel Indoleamine 2,3-Dioxygenase 1 (IDO1) and Histone
Deacetylase (HDAC) Dual Inhibitors. *ACS Med Chem Lett* **2018**, *9* (4), 312-317.
23. Zou, Y.; Wang, F.; Wang, Y.; Sun, Q.; Hu, Y.; Li, Y.; Liu, W.; Guo, W.; Huang, Z.;
Zhang, Y.; Xu, Q.; Lai, Y., Discovery of imidazoleisoindole derivatives as potent
IDO1 inhibitors: Design, synthesis, biological evaluation and computational
studies. *Eur J Med Chem* **2017**, *140*, 293-304.
24. Coluccia, A.; Passacantilli, S.; Famiglini, V.; Sabatino, M.; Patsilnakos, A.;
Ragno, R.; Mazzoccoli, C.; Sisinni, L.; Okuno, A.; Takikawa, O.; Silvestri, R.; La
Regina, G., New Inhibitors of Indoleamine 2,3-Dioxygenase 1: Molecular
Modeling Studies, Synthesis, and Biological Evaluation. *J Med Chem* **2016**, *59*
(21), 9760-9773.
25. Fang, K.; Wu, S.; Dong, G.; Wu, Y.; Chen, S.; Liu, J.; Wang, W.; Sheng, C.,
Discovery of IDO1 and DNA dual targeting antitumor agents. *Org Biomol Chem*
2017, *15* (47), 9992-9995.
26. Cheong, J. E.; Ekkati, A.; Sun, L., A patent review of IDO1 inhibitors for cancer.
Expert Opin Ther Pat **2018**, *28* (4), 317-330.
27. Peng, Y. H.; Ueng, S. H.; Tseng, C. T.; Hung, M. S.; Song, J. S.; Wu, J. S.; Liao, F.
Y.; Fan, Y. S.; Wu, M. H.; Hsiao, W. C.; Hsueh, C. C.; Lin, S. Y.; Cheng, C. Y.; Tu,

- C. H.; Lee, L. C.; Cheng, M. F.; Shia, K. S.; Shih, C.; Wu, S. Y., Important hydrogen bond networks in indoleamine 2,3-dioxygenase 1 (IDO1) inhibitor design revealed by crystal structures of imidazoleisoindole derivatives with IDO1. *J Med Chem* **2016**, *59* (1), 282-93.
28. Beatty, G. L.; O'Dwyer, P. J.; Clark, J.; Shi, J. G.; Bowman, K. J.; Scherle, P. A.; Newton, R. C.; Schaub, R.; Maleski, J.; Leopold, L.; Gajewski, T. F., First-in-human phase I study of the oral inhibitor of indoleamine 2,3-dioxygenase-1 epacadostat (INCB024360) in patients with advanced solid malignancies. *Clin Cancer Res* **2017**, *23* (13), 3269-3276.
29. Epacadostat shows value in two SCCHN trials. *Cancer Discovery* **2017**, *7* (9), OF2/1-OF2/2.
30. Li, M.; Bolduc, A. R.; Hoda, M. N.; Gamble, D. N.; Dolisca, S. B.; Bolduc, A. K.; Hoang, K.; Ashley, C.; McCall, D.; Rojiani, A. M.; Maria, B. L.; Rixe, O.; MacDonald, T. J.; Heeger, P. S.; Mellor, A. L.; Munn, D. H.; Johnson, T. S., The indoleamine 2,3-dioxygenase pathway controls complement-dependent enhancement of chemo-radiation therapy against murine glioblastoma. *J Immunother Cancer* **2014**, *2*, 21.
31. Marmarelis, M. E.; Aggarwal, C. Combination immunotherapy in non-small cell lung cancer. *Curr Oncol Rep* **2018**, *20* (7), 55.
32. Muller, A. J.; DuHadaway, J. B.; Donover, P. S.; Sutanto-Ward, E.; Prendergast, G. C., Inhibition of indoleamine 2,3-dioxygenase, an immunoregulatory target of the cancer suppression gene Bin1, potentiates cancer chemotherapy. *Nat Med* **2005**, *11* (3), 312-9.
33. Toulmonde, M.; Penel, N.; Adam, J.; Chevreau, C.; Blay, J. Y.; Le Cesne, A.; Bompas, E.; Piperno-Neumann, S.; Cousin, S.; Grellety, T.; Ryckewaert, T.; Bessede, A.; Ghiringhelli, F.; Pulido, M.; Italiano, A., Use of PD-1 targeting, macrophage infiltration, and IDO pathway activation in sarcomas: a phase 2 clinical trial. *JAMA Oncol* **2018**, *4* (1), 93-97.

34. Long, G. V.; Dummer, R.; Hamid, O.; Gajewski, T.; Caglevic, C.; Dalle, S.; Arance, A.; Carlino, M. S.; Grob, J.-J.; Kim, T. M.; Demidov, L. V.; Robert, C.; Larkin, J. M. G.; Anderson, J.; Maleski, J. E.; Jones, M. M.; Diede, S. J.; Mitchell, T. C., Epacadostat (E) plus pembrolizumab (P) versus pembrolizumab alone in patients (pts) with unresectable or metastatic melanoma: Results of the phase 3 ECHO-301/KEYNOTE-252 study. *Journal of Clinical Oncology* **2018**, *36* (15_suppl), 108-108.
35. Lewis-Ballester, A.; Pham, K. N.; Batabyal, D.; Karkashon, S.; Bonanno, J. B.; Poulos, T. L.; Yeh, S. R., Structural insights into substrate and inhibitor binding sites in human indoleamine 2,3-dioxygenase 1. *Nat Commun* **2017**, *8* (1), 1693.
36. Koblish, H. K.; Hansbury, M. J.; Bowman, K. J.; Yang, G.; Neilan, C. L.; Haley, P. J.; Burn, T. C.; Waeltz, P.; Sparks, R. B.; Yue, E. W.; Combs, A. P.; Scherle, P. A.; Vaddi, K.; Fridman, J. S., Hydroxyamidine inhibitors of indoleamine-2,3-dioxygenase potently suppress systemic tryptophan catabolism and the growth of IDO-expressing tumors. *Mol Cancer Ther* **2010**, *9* (2), 489-98.
37. Kottke, T.; Evgin, L.; Shim, K. G.; Rommelfanger, D.; Boisgerault, N.; Zaidi, S.; Diaz, R. M.; Thompson, J.; Ilett, E.; Coffey, M.; Selby, P.; Pandha, H.; Harrington, K.; Melcher, A.; Vile, R., Subversion of NK-cell and TNFalpha immune surveillance drives tumor recurrence. *Cancer Immunol Res* **2017**, *5* (11), 1029-1045.
38. Yue, E. W.; Douty, B.; Wayland, B.; Bower, M.; Liu, X.; Leffet, L.; Wang, Q.; Bowman, K. J.; Hansbury, M. J.; Liu, C.; Wei, M.; Li, Y.; Wynn, R.; Burn, T. C.; Koblish, H. K.; Fridman, J. S.; Metcalf, B.; Scherle, P. A.; Combs, A. P., Discovery of potent competitive inhibitors of indoleamine 2,3-dioxygenase with in vivo pharmacodynamic activity and efficacy in a mouse melanoma model. *J Med Chem* **2009**, *52* (23), 7364-7.
39. Buchholz, M.; Heiser, U.; Schilling, S.; Niestroj, A. J.; Zunkel, K.; Demuth, H. U., The first potent inhibitors for human glutaminy cyclase: synthesis and

- structure-activity relationship. *J Med Chem* **2006**, *49* (2), 664-77.
40. Wolfard, J.; Xu, J.; Zhang, H.; Chung, C. K., Synthesis of Chiral Tryptamines via a Regioselective Indole Alkylation. *Org Lett* **2018**, *20* (17), 5431-5434.
41. Dou, D.; Tiew, K. C.; He, G.; Mandadapu, S. R.; Aravapalli, S.; Alliston, K. R.; Kim, Y.; Chang, K. O.; Groutas, W. C., Potent inhibition of Norwalk virus by cyclic sulfamide derivatives. *Bioorg Med Chem* **2011**, *19* (20), 5975-83.
42. Yu, C. J.; Zheng, M. F.; Kuang, C. X.; Huang, W. D.; Yang, Q., Oren-gedoku-to and its constituents with therapeutic potential in Alzheimer's disease inhibit indoleamine 2, 3-dioxygenase activity in vitro. *J Alzheimers Dis* **2010**, *22* (1), 257-66.